# SUPERFLUID DRAG IN HELIUM II

Thesis by
John Philip Andelin, Jr.

In Partial Fulfillment of the Requirements

For the Degree of
Doctor of Philosophy

California Institute of Technology
Pasadena, California
1967
(Submitted May 26, 1966)

# ACKNOWLEDGMENTS

I would like to express my appreciation to Professor James E. Mercereau for his patient guidance and constant encouragement. I would also like to thank Professor R. P. Feynman for many stimulating and enlightening luncheon discussions. Special acknowledgment must be given to Professor John R. Pellam for the suggestion of this problem.

Financial assistance has been generously provided by the Hughes Aircraft Co., The National Science Foundation and the Alfred P. Sloan Foundation.

# ABSTRACT

The drag on a 1.21 millimeter diameter sphere due to flowing superfluid helium II was measured at 1.6°K, 1.8°K, 2.0°K and 2.13°K in a "superfluid wind tunnel" (test region 3 cm long and 1 cm diameter) in which 500 Å Millipore was used as the barrier to normal component flow for the first experiments, and 100 Å Millipore for the later ones. The superfluid flow through the tunnel was much steadier than it was in similar tunnels used in previous experiments. The velocity of the superfluid was calculated from a measurement of the loss rate of liquid helium in a standpipe at the entrance to the tunnel. (This design eliminated uncertainty in the corrections for evaporation.) The test sphere was mounted 1.3 cm from the axis of a quartz torsion fiber assembly, on which was also mounted a magnetic dipole. The drag was then measured using a null technique in which the torque due to the drag on the sphere in the flowing superfluid was balanced by the torque on the dipole due to an externally applied magnetic field. After corrections were made for a backflow of normal component which leaked through the Millipore, the results were as follows: Within the experimental error, zero drag was often observed for superfluid velocities up to 0.21 cm/sec at 1.6°K, 0.48 cm/sec at 1.8°K, 1.1 cm/sec at 2.0°K and 4.4 cm/sec at 2.13°K. (These velocities do not necessarily represent superfluid critical velocities, but they are probably limiting velocities imposed by the measurement technique.) At 2.13°K, only zero drag was observed, but at the other three temperatures, drag was also observed with steady values between zero and a drag comparable to

that which would be produced by an ordinary, low viscosity liquid having the density and velocity of the superfluid. These results are qualitatively consistent with the Onsager-Feynman model of quantized vortices, but the velocities at which zero drag was observed are much larger than quantitative predictions based on this model.

# TABLE OF CONTENTS

# LIST OF FIGURES

# I. INTRODUCTION[1]

Liquid $He^4$ undergoes a phase transformation at 2.172°K. The high temperature phase, called helium I, is an ordinary liquid having low viscosity and density. The low temperature phase, called helium II, is unlike any other liquid. For example, the viscosity of helium II obtained by measuring the damping of an oscillating disk is several orders of magnitude larger than that obtained by measuring the flow through thin channels. Some flow experiments have even indicated that the helium exhibits zero viscosity as long as its velocity is less than a critical velocity whose value depends on the type and geometry of the experiment.

The seemingly inconsistent results of viscosity measurements can be explained by a macroscopic, phenomenological theory based on a two-fluid model[2], which states that helium II is composed of two mutually interpenetrating fluids. One component, called the superfluid, possesses no entropy, and, at low velocity, no viscosity; the other, called the normal component, carries the entropy and is in all respects an ordinary fluid. The fraction of helium II which is superfluid is a unique and monotonic function of the temperature, such that the helium II is entirely superfluid at 0°K and all normal component at the transition temperature.

---

(1) A general reference for the entire paper is K. R. Atkins, Liquid Helium (Cambridge University Press, 1959).

(2) For a discussion of the evolution of the two-fluid model, see F. Landau, Superfluids, Vol II, p. 40ff (John Wiley and Sons, Inc., New York, 1954).

In 1941, Landau[3] extended the quantum theory of fields to liquid helium, treating it as a continuous fluid with quantized modes of motion. He showed that the mass and momentum of the normal component in the two-fluid model can be attributed to the total effective mass and momentum of the elementary excitations, and that the superfluid can be identified with the unexcited background helium. He calculated that the excitations he postulated could not be formed at superfluid velocities less than 70 m/sec. Unfortunately, this value for the critical velocity at which dissipation sets in was more than one hundred times larger than experimentally determined ones[4].

In 1955, Feynman[5] analyzed the motion of a Bose liquid and showed that vortices with quantized circulation[6] could exist in the superfluid, and would allow dissipation in superfluid flow at velocities well below Landau's critical velocity. He made a rough estimate of the critical velocity for vortex formation and obtained $v_c \sim (\hbar/md)\, \ell n\, (d/a)$, where m is the mass of a helium atom; d, the characteristic dimension of the flow; and a, the "core radius" of the vortex line, probably a few angstroms.

This expression qualitatively agrees with experimental results in the respect that it predicts critical velocities which

---

(3) L. Landau, J. Phys., Moscow, 5, 71 (1941); 11, 91 (1947).

(4) V. P. Peshkov, Progress in Low Temperature Physics, Vol.IV (edited by C. J. Gorter), Chapter I (North Holland Publishing Co., Amsterdam).

(5) R. P. Feynman, Progress in Low Temperature Physics, Vol. I (edited by C. J. Gorter), Chapter II (North Holland Publishing Co., Amsterdam).

(6) First suggested by L. Onsager, Nuov. Cim., 6 (Suppl. 2), 249 (1949).

decrease as the characteristic dimension of the flow increases. However, careful comparison of experimental values of critical velocities of superfluid flows and theoretical estimates made from the Onsager-Feynman vortex model shows that the experimental dependence of the critical velocity on the characteristic dimension is not as strong as $(\ell nd)/d$. Thus, the predicted value of the superfluid critical velocity is too high for flows in small channels[7], about right for flows with characteristic dimensions between $10^{-3}$ and $10^{-1}$ cm, and too small for flows with larger characteristic dimensions.[8, 9, 10] For example, the predicted critical velocity for film flow ($d \sim 300$ Å) is about 200 cm/sec, while the observed value is only 25 cm/sec.[11] In contrast, Reppy and Lane[9] rotated a 2.5 cm diameter cylindrical bucket and obtained a critical velocity of $10^{-1}$ cm/sec - forty times the theoretical value of $2.5 \times 10^{-3}$. In a similar experiment, Bendt[10] measured a superfluid critical velocity of 0.5 cm/sec for helium II in an annular region 2 cm long, 0.2 cm wide, with an average diameter of 9 cm. The theoretical critical velocity based on the 0.2 cm width is only $1.5 \times 10^{-2}$ cm/sec.

---

(7) See Reference 1, p. 199, or Reference 4, p. 24 for a summary of experimental critical velocities.

(8) P. P. Craig, Thesis, California Institute of Technology, 1959; P. P. Craig and J. R. Pellam, Phys. Rev. 108, 1109 (1957).

(9) J. D. Reppy and C. T. Lane, Proceedings of The Seventh International Conference on Low-Temperature Physics, p. 443 (University of Toronto Press, Toronto, 1960).

(10) P. J. Bendt, Phys. Rev. 127, 1441 (1962).

(11) J. G. Daunt, K. Mendelssohn, Proc. Roy. Soc. A 170, 423, 439 (1939).

One of the more interesting large dimension experiments on the flow of helium II was that done by Craig.[8] He investigated the lift on airfoils in the flow of a "superfluid wind tunnel". His tunnel consisted of glass tubing with a heater and packed carborundum seal arranged to drive the superfluid by the thermomechanical effect while restricting the flow of the normal component. Craig concluded that the lift due to the superfluid flow, and hence the viscosity of the superfluid, was identically zero for freestream superfluid velocities up to several millimeters/second. He also stated that the experimental lifts for velocities larger than the critical velocities could be fitted by a quadratic function of the superfluid velocity. Even at very high velocities, however, the experimental lift approached only 0. 13 to 0. 55 of the classical limit, depending on which airfoil was used.

The critical velocities reported by Craig are much larger than predicted from theory, but they are still reasonably consistent with those obtained in other large dimension flow experiments.[9, 10] The unexpectedly small lift in the high velocity region, however, has neither theoretical explanation nor experimental confirmation. In view of this result, it would seem prudent to look at Craig's experiment rather critically.

Craig states that he encountered some unexplained experimental problems. For example, the helium flow through the tunnel was so irregular that he had difficulty not only in measuring the superfluid velocity, but also in measuring the lift. In fact, before he could make any measurement of the lift at all, he had to use very heavy damping on his airfoil, thereby precluding the observation of short term forces. After damping his airfoil enough to make measurements, Craig observed negative lift when the superfluid velocity was less than critical. This was presumably due to some

of the normal component flowing in the direction opposite to the superfluid flow, but he states that the magnitude of the negative lift was much too large for any reasonable velocity of the normal component. Finally, Craig seems to have overlooked a large systematic error in his calibration procedure. He determined the torsion constant of a quartz fiber by measuring its period in air with a "known moment of inertia", but he did not correct for the probably large moment of inertia of the air which was dragged along by viscous forces, so he underestimated the actual forces. This may account for the comparatively small lift which he reported at high superfluid velocities. With these questions in mind, it was clear that additional investigations of the forces due to flowing helium II were necessary to clarify the experimental situation.

The present investigation first required that an improved "superfluid wind tunnel" be developed, one in which the superfluid flow is steady enough to allow accurate force measurements without requiring heavy damping of the measuring system, and in which the flow of normal component is eliminated, or, at least, understood and controlled. It also required that a more accurate technique for the measurement of the superfluid velocity be developed.

Once the improved tunnel was completed, and its flow properties understood, the next step was to calibrate the system accurately and measure the forces on an object immersed in the flowing helium II. It was decided to measure the drag on a sphere, since the shape is simple enough to allow an accurate calculation of the forces which would be expected from the flow of an ordinary viscous fluid. The measurement utilized a null technique in which the torque on the torsion pendulum due to the drag on the sphere was

balanced by the torque due to the interaction between an external magnetic field and a permanent magnetic dipole mounted on the pendulum.

Details of the apparatus and measuring technique will be described more fully, along with a presentation of the results. The experimentally observed forces due to the superfluid flow will be compared quantitatively with the forces calculated on the basis of ordinary viscous fluid flow. Significance of the results will be discussed in relation to other experiments and to theory.

# II. APPARATUS

## A. Design Considerations

### 1. General

A basic "superfluid wind tunnel" ordinarily consists of an intake, a test region, one or more semipermeable barriers, a heater and an exhaust. There must also be a provision for introducing the object to be observed into the test region and measuring the forces or torques on it, and, usually, some means of determining the superfluid velocity through the tunnel. In most previous experiments[10, 12], as well as the present one, the test object is attached to a thin support arm, which is, in turn, suspended on a torsion fiber. Under these conditions, the test object and support are held up against gravity, but are still relatively free to rotate about the vertical axis defined by the fiber, being restrained only by the torsion constant of the fiber.

Previous experiments with "superfluid wind tunnels" and torsion pendulum assemblies have been complicated by forces due to static electricity and to external vibration,[10] and by random variations in the flow rate of the helium.[10, 12] Preliminary experiments were performed to see if these problems could be eliminated or reduced.

---

(12) T. R. Koehler, Thesis, California Institute of Technology, 1960; T. R. Koehler and J. R. Pellam, Phys. Rev. 125, 791 (1962).

## 2. Stability of measuring apparatus

Static electricity was the biggest problem in the earliest "superfluid wind tunnel" built for this experiment. The only stable positions of the pendulum assembly (see Figures 1 and 2, pages 18 and 19 ) were with the sphere or support touching one of the walls of the test section. This problem was solved by making the pendulum assembly electrically conducting and limiting its motion with conducting stops.

After the forces due to static electricity were eliminated, the effects of external vibration could be studied by watching the motion of the pendulum in an evacuated dewar. With no special precautions to isolate the system from the floor and pump, the pendulum moved about erratically, occasionally going far enough to hit the stops, $10^{-1}$ radians apart. After vibration isolation, the maximum excursion of the pendulum was less than $10^{-3}$ radians. Typical drag forces observed in this experiment corresponded to deflections of $10^{-2}$ to $10^{-1}$ radians - smaller than the original noise. At this point, the system was completely stable in a vacuum or in quiescent helium II, so it was decided not to use any damping on the pendulum other than that due to the normal component of the helium II. Thus, small forces on the pendulum due to the flowing helium could be watched on a time scale comparable to the period of the pendulum, and larger forces, of course, could be observed on a considerably shorter time scale. This is in contrast to the heavily damped systems used in previous experiments[10, 12].

In the presence of flowing helium, the pendulum was again found to move about erratically. Most of the motion was due

to an unsteady superfluid flow through the tunnel, even though constant power was put into the exhaust heater. The irregular flow could be readily seen just by watching the liquid coming out of the exhaust. Previous helium II flow problems utilizing "superfluid wind tunnels" have also been complicated by this varying flow.[10, 12]

3. Stability of flow

In an effort to stabilize the superfluid flow through the tunnel, the material used to construct the semipermeable barrier was varied. Neither glass frit nor tightly packed carborundum was found at all suitable, not only because the superfluid flow in the tunnel was unsteady, but also because enough normal component flowed through them to produce drag forces on the pendulum assembly much larger than those which were expected from the superfluid flow. To the approximation required in this experiment, neither ultrafine glass frit nor packed carborundum could be considered superleaks.

The next material tried was packed jeweler's rouge, which, though quite effective in preventing the flow of normal fluid, did not solve the problem of an irregular superfluid flow. It was noticed, however, that the temperature drop across the rouge was several times the theoretical thermomechanical temperature difference. This implied that the superfluid was not flowing through the rouge freely - that it had exceeded its critical velocity in the rouge. So, to keep the superfluid velocity below critical for the same volume flow of helium, it would seem reasonable to increase the total area of the semipermeable barrier, increase the fraction of open area, or decrease the channel width so that the value of the critical velocity would increase.

The next tunnel was built with these guidelines and the superfluid flow through it was found to be much steadier. The area of the barrier was increased by a factor of four, and the channel size was decreased by changing the material from which the barrier was constructed from packed rouge, with an effective channel size of $10^3$ Å[13] to 500 Å Millipore[14]. Unfortunately, these presumed improvements were made at the same time, so it is impossible to tell their relative importance.

This 500 Å Millipore tunnel was used to determine the effect of the heater size on the stability of flow. It was constructed with three independent resistors, having surface areas of 0.18 $cm^2$, 5.6 $cm^2$ and 500 $cm^2$. They were used one at a time to run the tunnel. For a given power input, the flow of helium through the tunnel was considerably less steady when the smallest resistor was used than when either of the larger resistors were used. This was evidenced by larger, more erratic excursions of the pendulum and noticeable spurting of the liquid coming out of the exhaust of the tunnel. The behavior of the flow seemed the same for the medium resistor as for the large one. (The final tunnel had four independent heaters, each with a surface area of 2.8 $cm^2$. For electrical convenience, all four were used in series, even though the flow seemed just as steady with only one.)

---

(13) J. Reppy, J. Burnham, A. H. Spees and C. A. Reynolds, Proceedings of The Fifth International Conference on Low Temperature Physics and Chemistry, p. 30 (University of Wisconsin Press, Madison, 1958).

(14) Obtained from The Millipore Filter Corporation, Bedford, Mass. Specifications for the dimensions and porosity of Millipore are given by the Millipore Filter Corporation.

The last parameter which was investigated and found to have an effect on the stability of the superfluid flow was the shape of the exhaust nozzle. Several different shapes were tried. The nozzle which seemed to produce the least irregular flow, and which was chosen for the tunnel used for the drag measurements pointed $20^{o}$ above horizontal and had a smooth, flaring exit.

Even though the effect of different nozzles on the stability of flow was not large, it is believed that the most important remaining contribution to an irregular flow rate is the varying rate of evaporation of the helium from its exposed surface at the exhaust of the tunnel. The area of this surface changes with time when the liquid helium is flowing out of the exhaust, so the evaporation rate and heat loss also change. Since the input to the heater is constant, the net power available for the conversion of superfluid to the normal component will vary with time. This results in a changing flow of superfluid.

4. Determination of superfluid velocity

There is no completely satisfactory way to measure flow velocities in a "superfluid wind tunnel", even if the assumption is made that there is no leakage of normal fluid through the "semi-permeable" barrier. Craig[10] used a pitot tube in the helium II stream after the exhaust heater. Several people have caught the effluent helium stream in a bucket and timed the filling rate[12,15]. There are serious objections to both techniques.

---

(15) D. Y. Chung and P. R. Critchlow, Phys. Rev. Letters 14, 892 (1965).

The pitot tube method has an objection on theoretical grounds, since Bernoulli's equation for potential flow states that $(P + \rho v^2/2 + \rho gh)$ is a constant throughout the entire fluid, rather than just along a streamline, as in other flows. Thus, for irrotational flows, the liquid level in two static tubes having the same pressure at their surfaces will be at the same height, regardless of the fluid velocities at their bases. Even if rotation is allowed in the superfluid, and the pitot tube works normally, the height differences which would be produced with the flow rates used in this experiment would be in the range of 100 Å to 1 mm. These would be even harder to measure if, as Craig reported, the helium level were to bounce up and down several millimeters.

The bucket system has a different set of problems. A temperature difference across the semipermeable barrier is necessary to get a flow of helium by the fountain effect, so the helium on the exhaust side is warmer than the bath and will have a higher evaporation rate. The increased evaporation rate can be estimated to about $10^{-2}$ cc/sec. This is an error three times as large as the smallest volume flow rate used in this experiment and 10 - 20% of typical rates. In general, the bucket technique will measure a velocity which is less than the true velocity by an indeterminate amount.

A related problem is the narrow range of velocities over which bucket filling methods are applicable. If the filling time is appreciably longer than 100 seconds evaporation from the bucket becomes a significant fraction of the filling rate. Timing errors are fractionally large for filling times less than 5 seconds. Thus, the bucket technique is only useful for measuring velocities which differ by no more than a factor of about 20. The largest velocity in this experiment is 300 times the smallest.

The present system for determining velocities is related to the bucket method, but, since it avoids the problems due to evaporation, it greatly extends the useful range of velocities. Instead of measuring the amount of liquid helium caught in a bucket at the exhaust of the tunnel, the present technique measures the loss of liquid helium from a standpipe at the entrance to the tunnel (Figure 2, page 19). Though there is still evaporation, it is thermodynamically related to the total loss of helium from the standpipe (Appendix 1) and is accounted for in the calculation of the free stream superfluid velocity. Details of the measuring procedure are given in Section III-A.

B. Construction Details

The apparatus in the Dewar is functionally divided into three subunits -- "superfluid wind tunnel", torsion pendulum assembly and filler. The torsion pendulum assembly is shown in Figure 1. The sphere was formed by melting the end of a 0.15 mm quartz rod until the 1.21 mm sphere had formed. This made a smooth transition between the sphere and its support. The softest gas flame which would melt the quartz was used so that the surface tension of the quartz would be as high as possible and the deforming effects of the rapidly moving gas in the flame would be minimized. The counterbalance area of the pendulum is gold plated (Hanovia Liquid Bright Gold) and is kept between stops made of 0.025 cm diameter gold wire fastened to the bottom of the main chamber of the wind tunnel. This reduces the static electricity forces to such an extent that they can be neglected.

The magnetic dipole is an irregular piece of permanent magnet about 500 microns long and 50 microns in the transverse dimensions, weighing approximately 6 micrograms. It was placed in a 20 kilogauss field parallel to its long direction before being cemented to the quartz pendulum (Duco cement diluted 3:1 with acetone). While the cement was drying, the field from a small horseshoe magnet kept the magnetic dipole parallel to the quartz arm supporting the sphere.

The mirror is 1 mm square, 0.012 cm thick with evaporated aluminum on the front surface. The fiber is 2 cm long and 5 microns in diameter. It is attached to the top bracket and the pendulum with diluted Duco cement. The top bracket is made of #44 copper wire. After the pendulum assembly was completed, it was placed in a

magnetic field and the magnetic dipole moment was calibrated against the torsion constant of the fiber (See Section III-B). The dipole was then subjected to a 15 gauss AC field for a few minutes. The magnetic dipole moment was checked again and found unchanged. At no time after this was the dipole in a magnetic field larger than 3 gauss. The residual dipole moment was $8.7 \pm 0.2 \times 10^{-3}$ dyne cm/gauss. It had the same value when it was remeasured at the end of the experiment.

The "superfluid wind tunnel" (Figure 2) is made of Lucite sheet and tubing, cemented together with Weldon #3.[16] The volume of the main chamber is 179 $cm^3$. Electrical leads for the heater and temperature sensing resistors are #50 formvar coated copper wires brought through holes in the Lucite drilled with a #80 drill and filled with Resiweld #4 (1:1).[17] The Lucite and wires were cleaned with reagent grade acetone before being cemented. These cementing techniques have consistently produced systems with no superleaks. Millipore #1 cement[14] was used for joining Millipore to Lucite. Similar joints using pore-free Millipore were tested and found free of superleaks.

The Lucite plate to which the Millipore was cemented had twenty 6.3 mm diameter holes drilled through it. Thus, the exposed Millipore had an area of 6.2 $cm^2$ of which 70%, or 4.3 $cm^2$, consisted of pores, 130 $\mu$ long and $100 \pm 20$ Å diameter ($500 \pm 30$ Å for one series of measurements)[14]. The test region is 2.8 cm long and circular in cross section with a minimum area of 0.71 $cm^2$ where

---

(16) Manufactured by Industrial Polychemical Service, Gardena, California.

(17) Manufactured by H. B. Fuller Co., St. Paul, Minnesota.

the sphere is placed. The longitudinal profile is as shown in Figure 2. The ends were machined to smooth contours and the entire test region was polished to transparency.

The splash pan was designed to allow maximum evaporation of the helium from the filler, so that it could cool to the equilibrium vapor pressure before falling into the standpipe. The comb breaks the entering helium flow into many separate drops. This prevents the incoming helium from having a continuous fluid path from the splash pan to the helium level in the standpipe, thus eliminating second sound heat transfer. The standpipe has a cross sectional area of 3.28 $cm^2$.

The exhaust is a bent Lucite tube with 0.32 cm ID. (See Section II-B-3 for a discussion of design considerations.)

The heaters in the exhaust section of the "superfluid wind tunnel" and in the filler are made of 4 two watt 20 ohm carbon resistors (See Section II-B-3). Variable AC power is supplied to them with Variacs.

The temperature sensing resistors are Ohmite "Little Devil" 1/10 watt 5% 22 ohm resistors chosen to match at room temperature and nitrogen temperature to within 0.1%. See Appendix 2 for the technique and electronics used for measuring temperatures with carbon resistors.

One set of Helmholtz coils, outside the Dewar was used to cancel the vertical component of the earth's magnetic field. Another similar set, but with a horizontal field, was used to apply a known field to the dipole so the magnetic torque on it would balance any torque due to the drag on the sphere. Constant DC current is supplied to the vertical Helmholtz coils with a 12 v automobile battery and variable DC current to the horizontal coils with an H-labs 6200A DC power supply.

The entire Dewar and Helmholtz coil assembly is clamped rigidly to a table (total weight about 50 kg) which, for vibration isolation, is floating on three slightly inflated football bladders. Vacuum connection is made through thin wall brass bellows. The system of the table, Dewar and coils has a natural horizontal period of approximately 1 second and a vertical period of 1/3 second. (See Section II-B-2 for a discussion of the need for vibration isolation.)

The filler utilizes the fountain effect to raise the level of helium II in it above that of the main bath. It is made of Lucite sheet and tubing with 500 Å Millipore as the semipermeable barrier. The intake of the filler is near the bottom of the bath and the exhaust is in the splash pan of the superfluid wind tunnel. (The exhaust of the filler is shown schematically in Figure 2.)

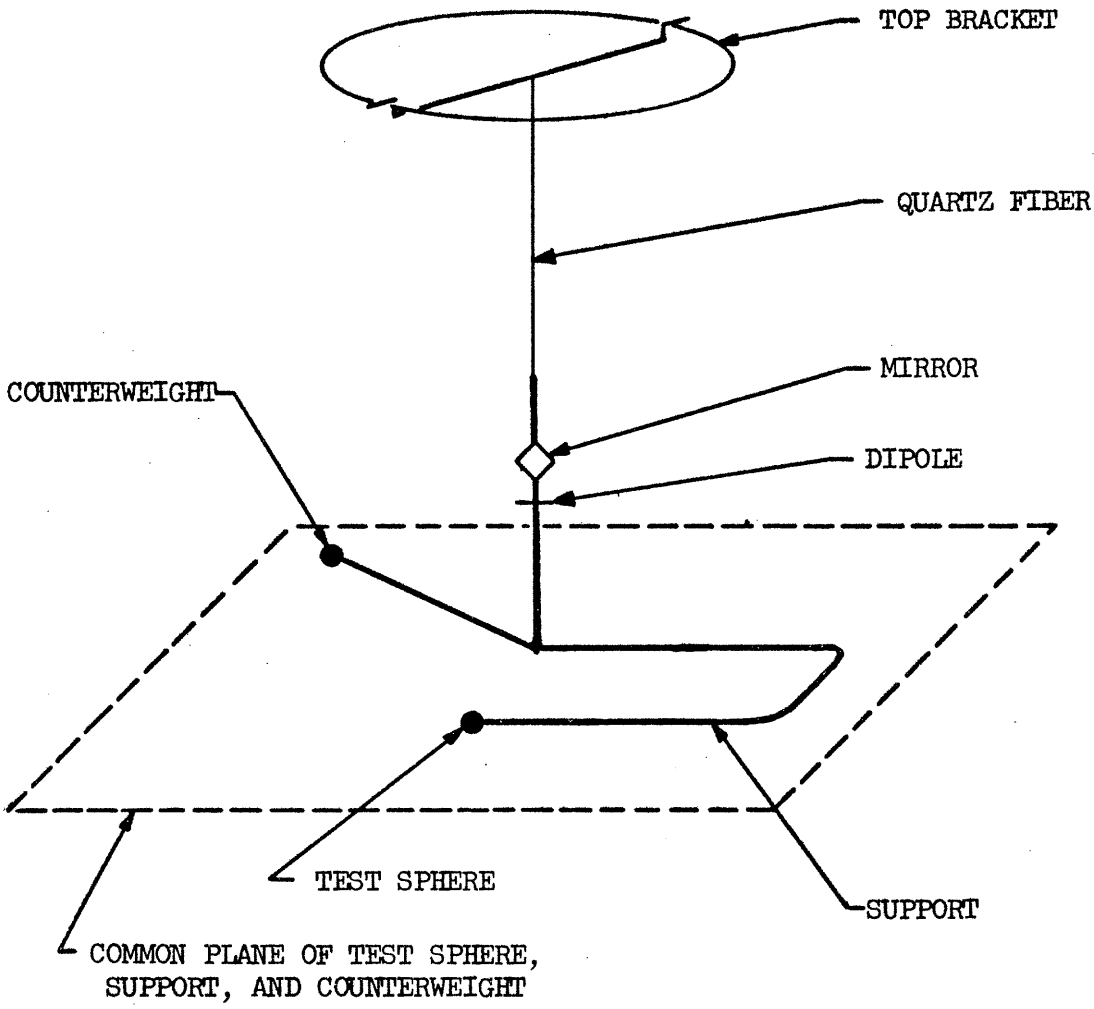


FIGURE 1. Torsion pendulum assembly.

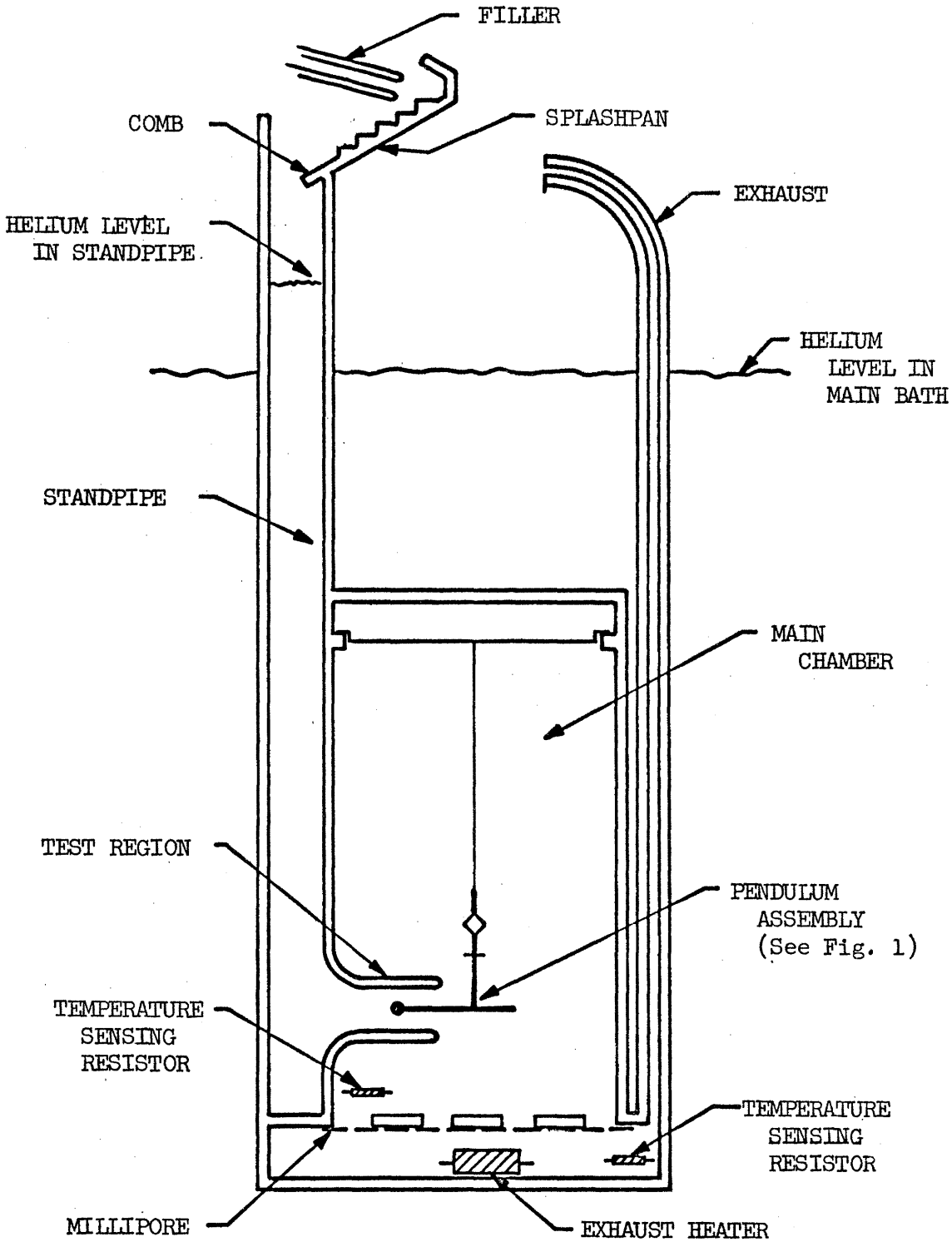


FIGURE 2. "Superfluid wind tunnel"

# III. PROCEDURE

## A. General

The data presented in this paper were taken during two series of runs, one with 500 Å Millipore as the barrier to the flow of the normal component ( 22 December 1965 to 4 January 1966) and one with 100 Å Millipore ( 15 February 1966 to 8 March 1966). Except for the change of Millipore, all the apparatus was the same in both series. At the start of each series of runs, after the complete tunnel assembly was put into the dewar, the dewar was evacuated for a day, flushed with helium gas, reevacuated and again filled with helium gas. The tunnel was then slowly cooled and kept in a helium atmosphere at or below $77^{\circ}$K until the entire series of runs was completed. In this way, it was hoped to prevent any changes in the properties of the Millipore due to contamination or thermal cycling.

A null technique was used to measure the drag on the sphere, so that the sphere would always be in the same position in the test region. The torque due to the drag on the sphere was balanced by the torque on the dipole in the magnetic field of the Helmholtz coils. Small deviations from null were watched by means of a slit of light bounced off the mirror and projected onto a screen. Angular motions of $10^{-3}$ radians could be resolved, corresponding to linear displacements of the sphere of 10 microns.

The heating effect of the measuring light has significantly affected the results of other helium flow experiments,[18] so

---

(18) D. S. Tsakadze and L. G. Shanshiashvili, JETP Letters 2, 194 (1965).

precautions were taken to see that this did not happen in the present experiment. The laboratory lights were kept off at all times during a run so the operator's eyes would be dark adapted. Then, the helium level and the position of the pendulum could be measured with relatively weak light sources. An entire day's run was spent investigating possible effects of the measuring lights and shorter checks were made on several other occasions. The light projected on the mirror was intentionally increased to five times its normal intensity for several minutes with no observable effect on the drag. This measuring light was also turned off for several minutes to see if the drag would change during the blackout. It never did. The light used to measure the helium level was checked in the same manner and it too was found to have no effect on the drag.

Most runs were made in the following way: Liquid helium was transferred into the dewar, and was pumped on until its vapor pressure, measured with a dibutyl phthalate manometer, corresponded to the temperature chosen for that run. The pressure above the helium bath was controlled by pumping through a condom regulator. The maximum pressure fluctuation during a run corresponded to a temperature shift of $0.003^{\circ}$. As soon as the helium was below the $\lambda$-point, the filler was used to transfer helium into the wind tunnel. When the main chamber and standpipe were full, the filler was turned off and the system was allowed to sit quietly for times up to 30 minutes. (Whether the measuring lights were on or off during the waiting period did not seem to have any effect on the subsequent measurements of the drag on the sphere.) The heater in the exhaust of the tunnel was then turned on, causing a net flow of helium from the standpipe, through the test region and Millipore, up the exhaust tube and into the bath. The position of the pendulum was

observed and recorded from the time the exhaust heater was turned on until either the pendulum stopped moving or the standpipe emptied of liquid helium. The current to the horizontal Helmholtz coils was adjusted until the average position of the pendulum was the same as its no-flow position.

The helium level in the standpipe was recorded as a function of time. With the exhaust heater off, the rate of change of the helium level in the standpipe was experimentally found to be negligible compared to the lowest velocities actually used. (This evaporation rate is considerably less than that of the main bath because the main bath shields the standpipe from conduction and radiation loss.) When the heater was on, the evaporation from the standpipe increased greatly but this evaporation is thermodynamically related to the total loss of helium from the standpipe (Appendix 1) and is accounted for in the calculation of the free stream superfluid velocity (Equation 6).

Some of the measurements were taken with the filler adding helium to the standpipe continuously at that rate which kept the level constant. It was found, however, that, especially at low superfluid velocity, both the absolute value of the drag and the fluctuations about its average were increased when the filler was used, indicating that turbulence was being generated in the flow by the liquid dripping from the comb into the helium II already in the standpipe. This was thought to be undesirable, because it might mask turbulence or dissipation due to flow past the sphere. Hence, the filler was usually left on continuously only for those velocities so high that the standpipe would otherwise empty before a drag measurement could be made. In this case, a different technique was used to determine the superfluid velocity. (At the highest velocity, the standpipe emptied in about 30 seconds, whereas a measurement of drag required several

minutes to complete.) The helium was added to the standpipe by continuously running the filler during a drag measurement, keeping the helium level in the standpipe constant. Then, after the drag measurement was completed, the filler was turned off and the helium level in the standpipe recorded as a function of time. Thus, for these high velocities, the drag and the superfluid velocity were determined, under essentially identical conditions, but at different times.

Some measurements were made with the sphere in a counterflow of normal fluid and superfluid helium rather than in the usual predominately superfluid flow. This was done by applying heat directly into the main chamber on the same side of the Millipore as the sphere and test region.

The variables recorded during each measurement were the time, current to the Helmholtz coils, position of the pendulum, power to the exhaust heater, helium level in the standpipe, and, during a few of the first runs, the helium level in the main bath. (It was found that the helium level in the main bath was unimportant, so it was not recorded during the later runs.) The time and the level of liquid helium in the standpipe can be used to calculate the rate of change of the helium level in the standpipe, v. Appendix 1 discusses the relation of v to the average free stream superfluid velocity in the test region, $\bar{v}_s$.

B. Calibration of Fiber and Dipole

The pendulum was placed in an evacuated chamber in a field-free region and its period in torsion measured to be $46.1 \pm 0.1$ sec. A known moment of inertia was added and the new period measured. The torsion constant of the fiber was computed from these measurements, and is $3.76 \pm 0.1 \times 10^{-4}$ dyne cm/radian. It should be pointed out that it is crucial to measure the period in a vacuum when using such lightweight and long period systems. When the present system was measured in air, the moment of inertia of the air dragged along with the pendulum was about three times as large as the moment of inertia of the pendulum itself. If the "known moment of inertia" from which the torsion constant is calculated were taken to be that of the pendulum assembly alone, the torsion constant would appear to be only one fourth of its actual value, and the forces measured in the experiment would seem proportionately too small.

The magnetic moment of the dipole (magnitude and direction) was determined by applying a magnetic field and observing the deflection of the pendulum and its period. The dipole direction was taken to be that of the external field when there was no angular change on applying the field. The external field was known to $\sim 1/2^{\circ}$. The most accurate technique for measuring the magnitude of the dipole was to measure the period of the pendulum for small oscillations in the presence of a magnetic field. Under these circumstances, the effective torsion constant, $k'$, is $(k + mB \cos \theta)$ where $k$ is the torsion constant of the fiber, $m$ the magnetic moment of the dipole, $B$ the external field and $\theta$ the angle between the dipole and field; the period is $2\pi\sqrt{(I/k')}$, where $I$ is the moment of inertia of the pendulum. (Note that $k'$ can be made smaller than

k if $|\theta| > 90^{o}$. This means that, for a given effective torsion constant, a torsion fiber with a dipole can be thicker than one without, and thus have a higher breaking strength. Further, the torsion constant, k', can be changed over a wide range during an experiment.) The magnetic moment of the dipole used in this experiment was $8.7 \pm 0.2 \times 10^{-3}$ dyne cm/gauss.

The effective torsion constant was calculated for a given B field from the fiber's torsion constant and the magnetic dipole moment.

To see whether the system was working properly, the drag of helium gas on the sphere and support, D, was measured at $77^{o}$K as a function of the time and total pressure, P, while the Dewar was slowly evacuated.

Under these conditions, the flow through the Millipore is negligible. Thus, all the gas which leaves the main chamber goes through the test region (see Figure 2). Assuming that the process is isothermal, the flow rate in the test region, $\bar{v}$, can be determined[19].

The largest Reynolds number (see Appendix 3) for the test region for the actual pressures and pumping rates used is $\sim 0.5$.

---

(19) The number of atoms which leave the main chamber per second is $(n/V)\,\bar{v}\,a$, where V is the volume of the main chamber, n is the number of atoms in V, a is the cross sectional area of the test region and $\bar{v}$ is the velocity of the helium gas in the test region, averaged over the cross section. From the perfect gas law, $PV = nkT$,

so, $$\frac{dn}{dt} = \frac{V}{kT}\frac{dP}{dt} = \left(\frac{n}{V}\right)\bar{v}\,a$$

This gives $$\bar{v} = \left(\frac{V}{a}\right)\left(\frac{1}{P}\frac{dP}{dt}\right).$$

This means that the flow is completely dominated by the viscosity and the drag should be linearly proportional to the velocity; $D(\bar{v})^{-1}$ was experimentally constant to 6% over a pressure range of 1 - 500 millibars and pumping rates, dP/dt, varying by a factor of three hundred.

A quantitative comparison can be made between the experimental results and theoretical predictions. At the highest velocity, the measured drag was 253 microdynes. Calculations from the experimental drag coefficients in Hoerner[20], neglecting interference drag or wall effects, give 154 microdynes for the support arm and 71 microdynes for the sphere, for a total of 225 microdynes. For such low Reynolds numbers, interference effects should be small, but the 13% difference is the right order of magnitude for wall effects. (The drag on the support arm, explicitly including wall effects, may be approximated by calculating the viscous drag on the center cylinder of a coaxial tube. This gives 176 microdynes, 15% higher than the value calculated from the drag coefficients in Hoerner[20].)

---

(20) S. F. Hoerner, Fluid-Dynamic Drag, 1965 edition (available from the author, 148 Busteed Dr., Midland Park, N. J.).

C. Flow Rate of Helium I Through Millipore

Flow rates through the pieces of 500 Å and 100 Å Millipore actually used in this experiment were measured with the Millipore cemented in place. Helium I was used at 4.2°K with a pressure head of $3.6 \times 10^3$ dynes/cm$^2$. The flow rate for the 500 Å Millipore under these conditions was $1.3 \pm 0.2 \times 10^{-2}$ ml/sec per square centimeter of Millipore; for the 100 Å Millipore, $0.32 \pm 0.05 \times 10^{-2}$ ml/sec/cm$^2$. With the assumption that the flow is linearly proportional to the pressure and inversely proportional to the viscosity, the flow rates of water through Millipore, given in the Millipore catalogue, can be compared to those measured for helium I. The helium I flow through the 500 Å Millipore is 30% higher than would be expected from the scaled flow of water; for the 100 Å Millipore, 20% higher. These differences cannot be considered significant in view of the 15% uncertainty in the helium measurement and a 20% uncertainty in the flow rates for water given in the Millipore catalogue.

## D. Correction Procedure

### 1. Normal Component Drag

At very low velocities, the drag is steady (to about $\pm$ 1 microdyne) and in the opposite direction to the superfluid flow. For example, the low velocity raw data taken at 1.8°K with 500 Å Millipore in the tunnel are shown in Figure 3, in which the observed drag is plotted against the rate of change of the helium level in the standpipe. The points taken with the filler turned off are represented by circles; those with the filler on, by crosses. The negative drag in the low velocity region is caused by backward leakage of normal component from the exhaust region through the pores in the Millipore. The rate of this leakage is proportional to the pressure drop across the Millipore, which, in turn, is proportional to the difference in height, $\Delta h$, between the helium level in the standpipe and in the exhaust. Thus, since the normal component's velocity is proportional to $\Delta h$, information about its drag can be obtained by plotting the negative drag data against $\Delta h$ (Figure 4). If the superfluid exerts any drag, the observed net drag will be less negative than it would be for the normal component alone. Hence, the lower envelope of the points in Figure 4, consistent with the error bars, represents a minimum value of the normal component drag as a function of $\Delta h$, and is fitted with a solid line.

If the velocity of the backflowing normal component is known as a function of $\Delta h$, the experimental curve, represented by a solid line in Figure 4, can be compared to theoretical estimates of the negative drag. An estimate of the numerical relation between the normal component velocity and $\Delta h$ can be obtained by extrapolating the experimental value for the flow rate of helium I at 4.2°K through

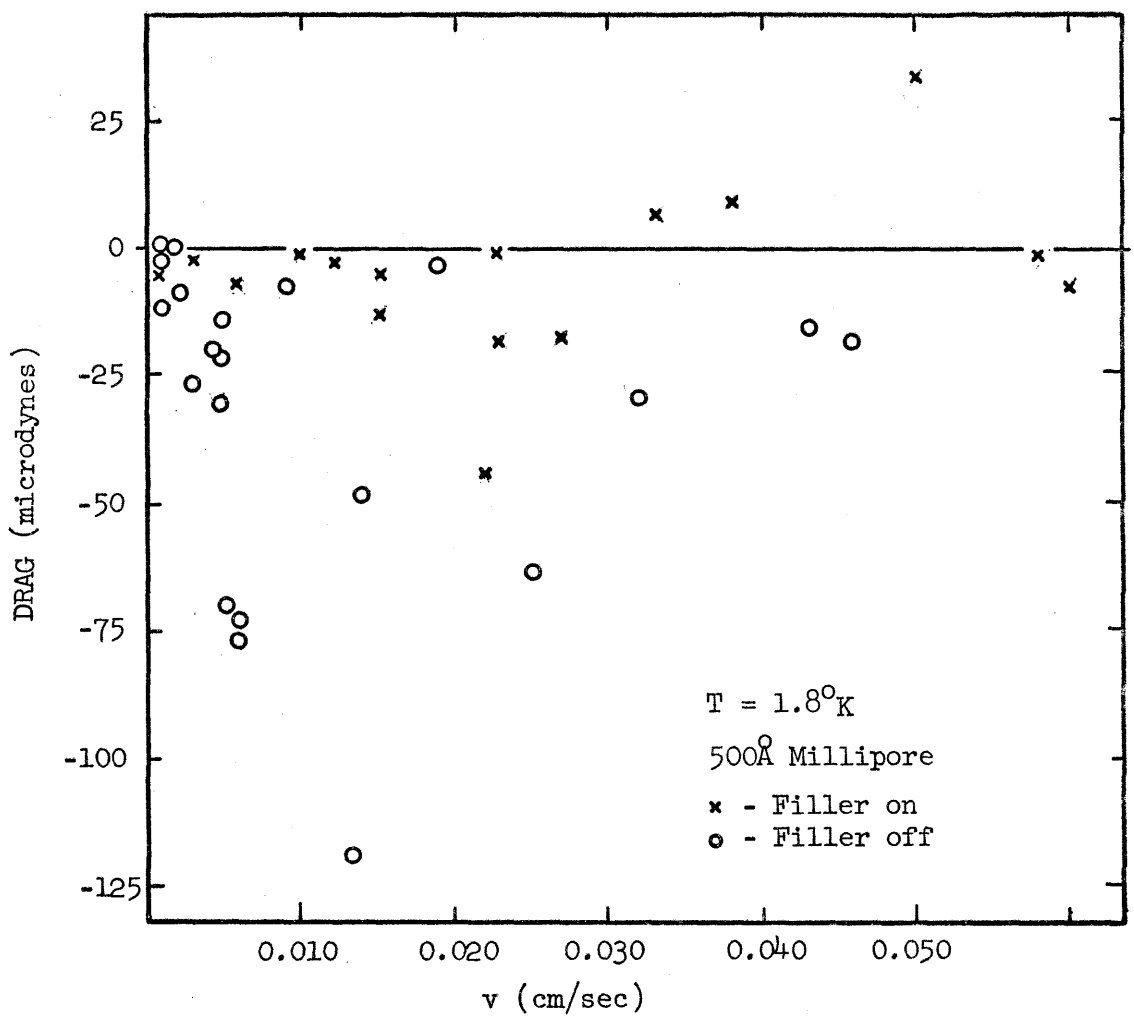


FIGURE 3. Drag on the sphere (uncorrected data) versus rate of change of helium level in standpipe.

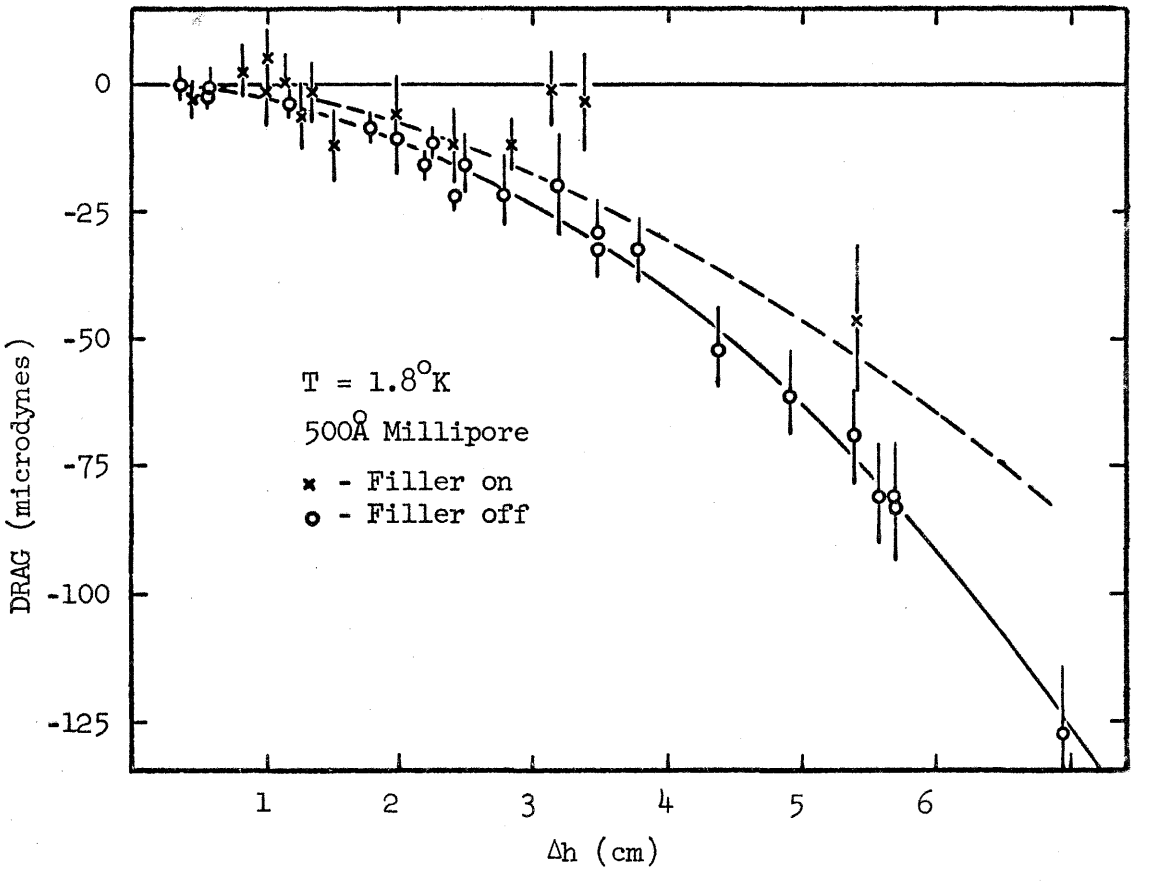


FIGURE 4. Drag on the sphere versus helium head, Δh. (Δh is the difference in height between the helium levels in the standpipe and in the exhaust.) Solid curve is the lower envelope of the data, consistent with the error bars. Dashed curve is a theoretical estimate of the drag (See Section III-D).

500 Å Millipore (Section III-C) to a pressure head of one centimeter of helium (140 dynes/$cm^2$) and to the viscosity of the normal component of helium II at 1.8°K (12 micropoise). This becomes 0.029 $cm^3$/sec, corresponding to a normal component velocity of 0.041 cm/sec in the test region, averaged over the cross section.

The drag on the sphere and support was estimated for a normal component velocity of 0.041 ($\Delta$h) cm/sec from published values of drag coefficients[20] after making approximate corrections for wall effects. This estimated drag is shown as a broken line in Figure 4, from which it can be seen that, for a given $\Delta$h, the theoretical estimate is about 70% of the value of the experimental curve. In view of the approximations made in the calculation, this agreement seems reasonable. It is somewhat better when the adjusted values of the normal component velocity to be described in Section III-D-2 are used.

Plots of the negative drag versus $\Delta$h were also made for the low velocity 100 Å data taken at 1.6°K, 2.0°K and 2.13°K. The lower envelopes, consistent with the error bars, are shown as solid lines in Figures 5A, 5B and 5C. Theoretical estimates of the normal component drag were made by the same procedure as that used for the 500 Å Millipore at 1.8°K, with those values of the normal component velocity and viscosity appropriate for the 100 Å Millipore at each temperature. These theoretical estimates are shown as dotted lines in Figures 5A, 5B and 5C , from which it can be seen that, in contrast to the 500 Å situation, the theoretical estimates are about 120% of the experimental values. As in the 500 Å case, agreement becomes better when adjusted values are used for the normal component velocities (Section III-D-2).

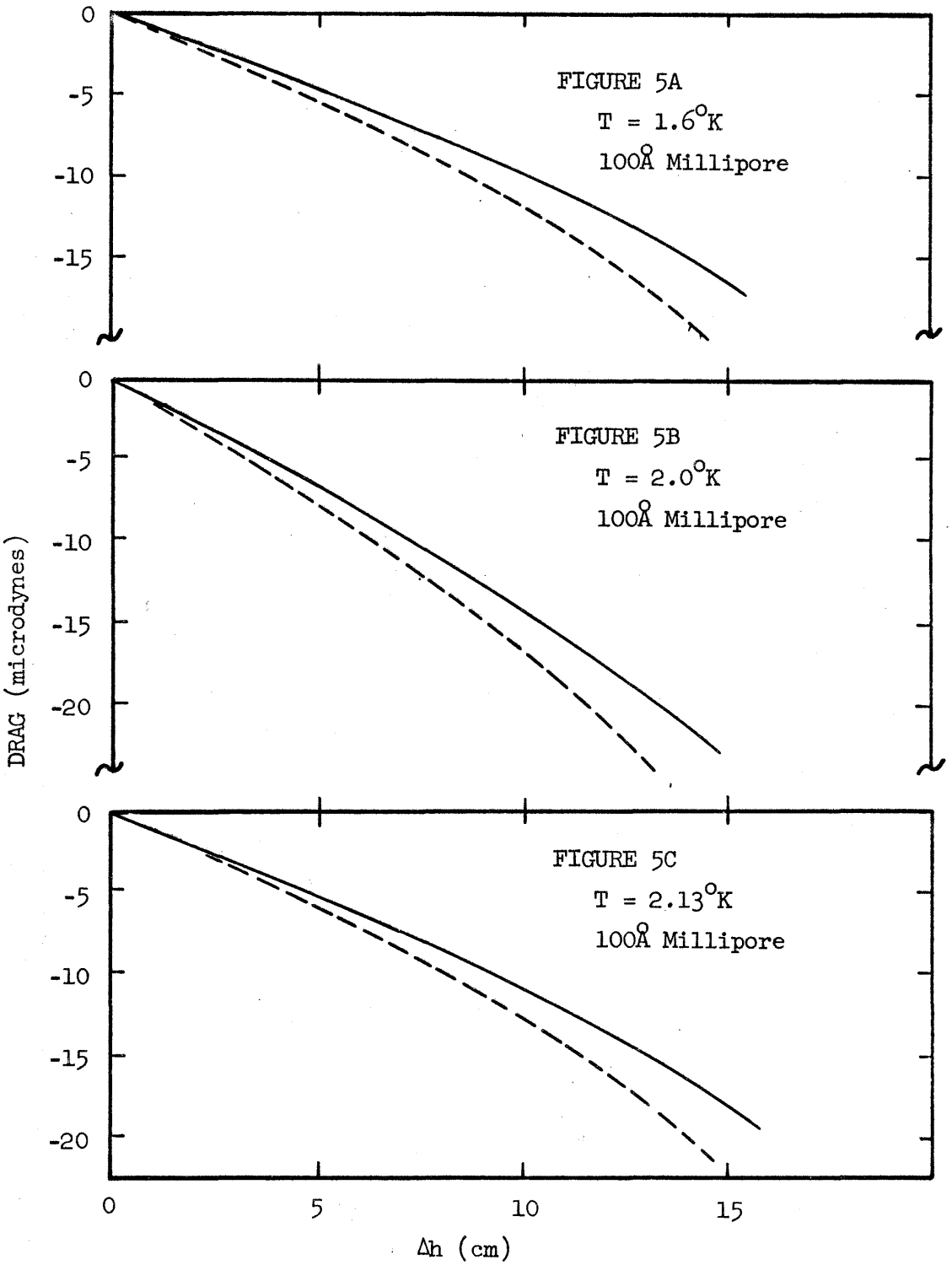


FIGURE 5. Correction curves for drag measured in the tunnel with 100Å Millipore. Solid curves are experimental, dashed curves are theoretical (See Section III-D).

2. Normal Component Velocity, $\bar{v}_n$

The normal component velocities used in the computation of the dotted curves in Figures 4 and 5 were determined by extrapolating experimental flow rates of helium I through 500 Å and 100 Å Millipore (Section III-D-1). Though the extrapolation procedure is likely to be quite accurate, the original flow rates were only determined to ± 15%, so comparable errors are possible in the values of the normal component velocity. These estimates of normal component velocities can be somewhat improved by means of the information contained in the agreement, or lack thereof, between the theoretical and experimental curves of Figures 4 and 5. ( Since there are undoubtedly some systematic errors in the calculation coming from interference drag and the wall effect corrections, the lack of agreement between the theoretical estimates for the drag and the experimental values cannot be used directly as a basis from which to calculate absolute values of the normal component velocities. However, the difference between the agreement for the 500 Å Millipore and the agreement for the 100 Å Millipore can be used indirectly to adjust the normal component velocities obtained from the extrapolation.)

Looking first at the curves for the tunnel with 100 Å Millipore, it can be seen that the ratio of the theoretical estimates to the experimental values is the same to a few percent for all three temperatures. Thus, it would seem that the temperature dependence in the theoretical drag calculation is essentially correct. Then, since the same physical situation is present in the test region whether the normal component leaks through 500 Å Millipore or 100 Å Millipore, and the calculation is the same for both cases, the ratio of theoretical estimates to experimental values should be the same for

the tunnel with 500 Å Millipore as for the tunnel with 100 Å Millipore. The fact that the ratios are different, (0.7 for 500 Å, 1.2 for 100 Å), implies an inconsistency in the value used for the normal component velocity in the 500 Å tunnel when compared to the values used in the 100 Å tunnel. In order to eliminate this discrepancy, a unique proportionality between the flow rates through 500 Å Millipore and through 100 Å Millipore must be assumed. This proportionality can then be used in conjunction with the numerical values for the normal component velocities obtained from the extrapolation to get adjusted values for the normal component velocities. The adjusted values of $\bar{v}_n$ are changed by about 10% from the original extrapolated values, and their error is reduced to $\sim$ 10%. For the 500 Å Millipore at 1.8°K, the adjusted value of the normal component velocity in the test region, averaged over the cross section, is $\bar{v}_n = 0.045\ (\Delta h)$, where $\bar{v}_n$ is in cm/sec and the helium head, $\Delta h$, is in centimeters. Similarly, for the 100 Å tunnel, $\bar{v}_n\ (1.6^{\circ}K) = 9.6 \times 10^{-3}\ (\Delta h)$; $\bar{v}_n\ (2.0^{\circ}K) = 8.9 \times 10^{-3}\ (\Delta h)$; $\bar{v}_n\ (2.13^{\circ}K) = 5.7 \times 10^{-3}\ (\Delta h)$; $\bar{v}_n\ (2.15^{\circ}K) = 5.2 \times 10^{-3}\ (\Delta h)$; and $\bar{v}_n\ (2.163^{\circ}K) = 5.0 \times 10^{-3}\ (\Delta h)$.

If these values for $\bar{v}_n$ are used to calculate drag curves for the normal component, they agree with the solid (experimental) curves in Figures 4 and 5 to within 5%.

### 3. Net Drag and Superfluid Velocity, $\bar{v}_s$

Each drag measurement can now be corrected for the normal component backflow due to helium head. For the data taken with 500 Å Millipore at 1.8°K and that taken with 100 Å Millipore at 1.6°K, 2.0°K and 2.13°K, the helium head at which the original measurement was made is converted to the normal component drag

represented by the appropriate solid (experimental) curve in Figure 4, 5A, 5B or 5C, and this drag is added to the original datum. For the data taken with 100 Å Millipore at 2.15°K and 2.163°K, the theoretical drag of the backflowing normal component due to the helium head is added to the measured drag. (21)

The superfluid velocity at which each measurement was taken was calculated from Equation 6, page 64. As explained in Part B of Appendix 2, the free stream superfluid velocity in the test region, $\bar{v}_s$, depends primarily on the rate of change of the helium level in the standpipe, v, but must also be corrected for the average normal component velocity in the test region, $\bar{v}_n$. Since the helium level in the standpipe was observed as a function of time, v is obtained directly from the original data; $\bar{v}_n$, however, must be determined indirectly, as explained in Section III-D-2. The adjusted values of $\bar{v}_n$ listed in Section III-D-2 were used in Equation 6 to calculate $\bar{v}_s$.

---

(21) The experimental procedure to correct for the helium head which was used at 2.13°K and below could not be used on the data at 2.15°K and 2.163°K, because, at the high temperatures, negative drag was observed which depended on the rate of change of the helium level in the standpipe as well as on the helium head. However, using the adjusted values for the normal component velocity given in Section III-D-2, the theoretical estimates of the negative drag due to the helium head at 1.6°K, 2.0°K and 2.13°K, are within 5% of the experimental values, so it was decided to use the theoretical estimates of the normal component drag at 2.15°K and 2.163°K as approximate corrections. It should be emphasized that these corrections do not significantly change the interpretation of the results at these two temperatures.

# IV. RESULTS

## A. Temperature Measurements

The temperature difference across the Millipore was measured with an accuracy of $3 \times 10^{-4}$ degrees (see Appendix 2) between 1.6°K and 2.163°K, with representative power inputs to the exhaust heater. At all temperatures below 2.14°, the temperature difference observed corresponded to the fountain effect $\Delta T$ required to support the extra head of helium on the exhaust side. Above 2.14°K, however, an extra temperature difference appeared as the power to the heater was increased. As an example of this, the data taken at 2.163°K are shown in Figure 6, where the extra temperature difference is plotted against the power input to the exhaust heater.

It can be inferred from this that below 2.14°K the Millipore is a "good" semipermeable barrier and the superfluid is flowing through it in an essentially thermodynamically reversible manner. The data taken below 2.14°K will be considered separately from that taken above 2.14°K.

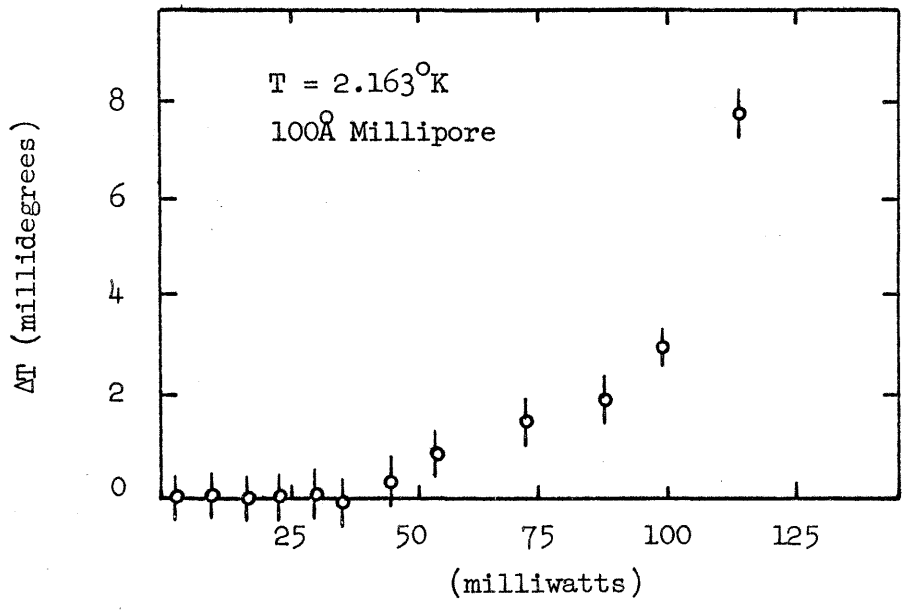


FIGURE 6. Extra temperature drop across Millipore versus power to the exhaust heater. T = 2.163°K.

## B. "Ideal" Superfluid Flow ($T < 2.14^{\circ}K$)

### 1. Results

The data taken at $1.8^{\circ}K$ with 500 Å Millipore in the tunnel were corrected for the normal component backflow due to helium head according to the procedure described in Section III-D, and are shown in Figure 7. (See Appendix 4 for a table of the original data.) The dotted curve is the drag due to a fluid having the density and velocity, $\bar{v}_s$, of the superfluid, with a drag coefficient of 0.5 (see Appendix 3).

In the low velocity region, the uncertainty of the measured drag is usually smaller than the uncertainty in the correction for the normal component drag due to helium head. This means that the error bars on the corrected drag represent the correction procedure rather than the measuring process. For most of the data, this uncertainty is large enough to cause doubt as to whether or not the superfluid drag at these low velocities is less than that represented by the dotted curve in Figure 7. It was decided to switch to 100 Å Millipore, with the expectation that the normal component backflow, and thus the negative drag correction, would be less than with 500 Å Millipore in the tunnel. (The data portrayed in Figures 5A, 5B and 5C were taken after the switch to 100 Å Millipore. They show that the normal component backflow is, in fact, much less at a given height for a tunnel with 100 Å Millipore than for a tunnel with 500 Å Millipore.)

The data taken at $1.6^{\circ}K$, $2.0^{\circ}K$ and $2.13^{\circ}K$ with 100 Å Millipore in the tunnel were corrected for the normal component backflow due to helium head according to the procedure described in Section III-D, and are shown in Figures 8 - 11. (Both Figure 9

and Figure 10 show data taken at 2.0°K. Figure 9 shows all the data; Figure 10 shows the low velocity data in greater detail.) (See Appendix 4 for a table of the original data.) The dotted curves in Figures 8 - 11 represent the drag due to a fluid having the density and velocity, $\bar{v}_s$, of the superfluid, with a drag coefficient as shown in each figure.

The time variation of the position of the pendulum depended on both the superfluid velocity through the test region and on the average value of the superfluid drag exerted on the sphere and support. At low superfluid velocities, the superfluid drag was always small, and any motions of the pendulum which might have been present were too small to be seen. In the region of moderate and large superfluid velocities, the motion of the pendulum depended strongly on the average value of the drag, being fairly steady at low drag and becoming more and more erratic at higher drag. An interesting type of behavior was sometimes seen in the region of moderate superfluid velocities ($\sim$ 0.3 cm/sec at 1.6°K and 1.0 cm/sec at 2.0°K, for example). The pendulum seemed to execute damped oscillatory motion about some value of the drag for several periods (roughly the same period as the natural period of the pendulum in the magnetic environment present at the time), and would then move away fairly rapidly, sometimes to repeat the damped oscillations about a new value of the drag. No preferred values of drag were observed.

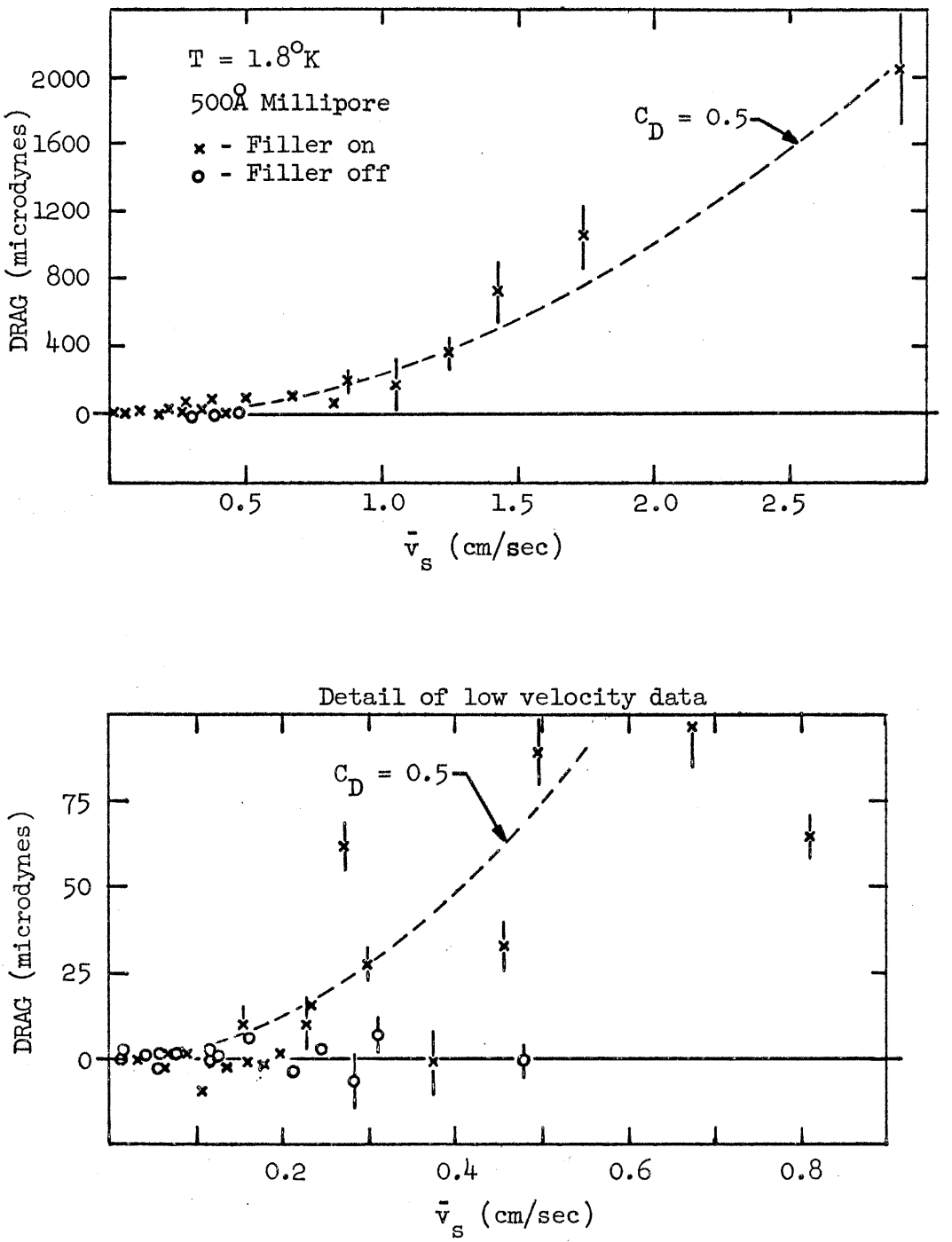


FIGURE 7. Drag on the sphere versus superfluid velocity in the test region, averaged over the cross section. T = 1.8°K. 500Å Millipore.

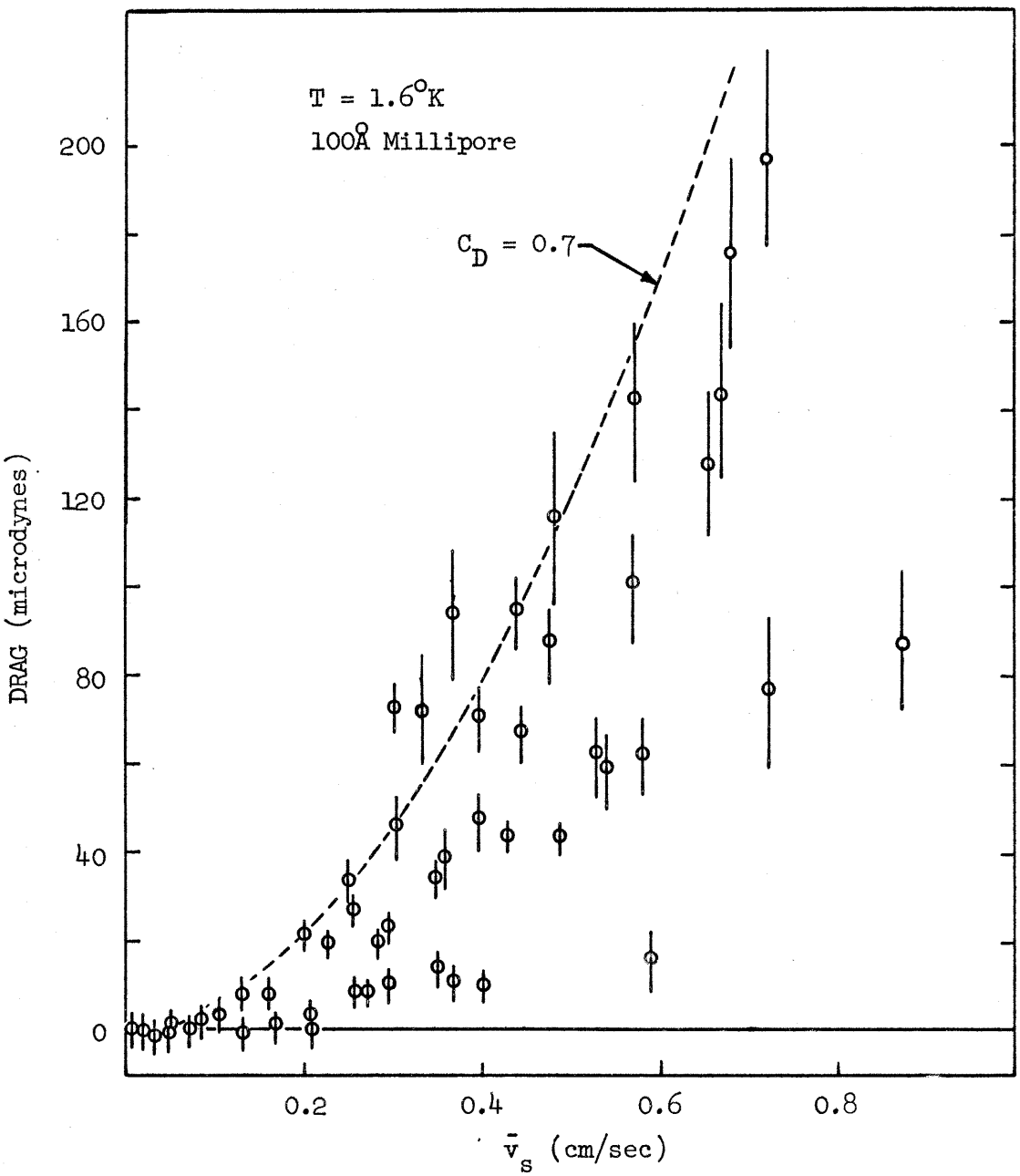


FIGURE 8. Drag on the sphere versus superfluid velocity in the test region, averaged over the cross section. T = 1.6°K.

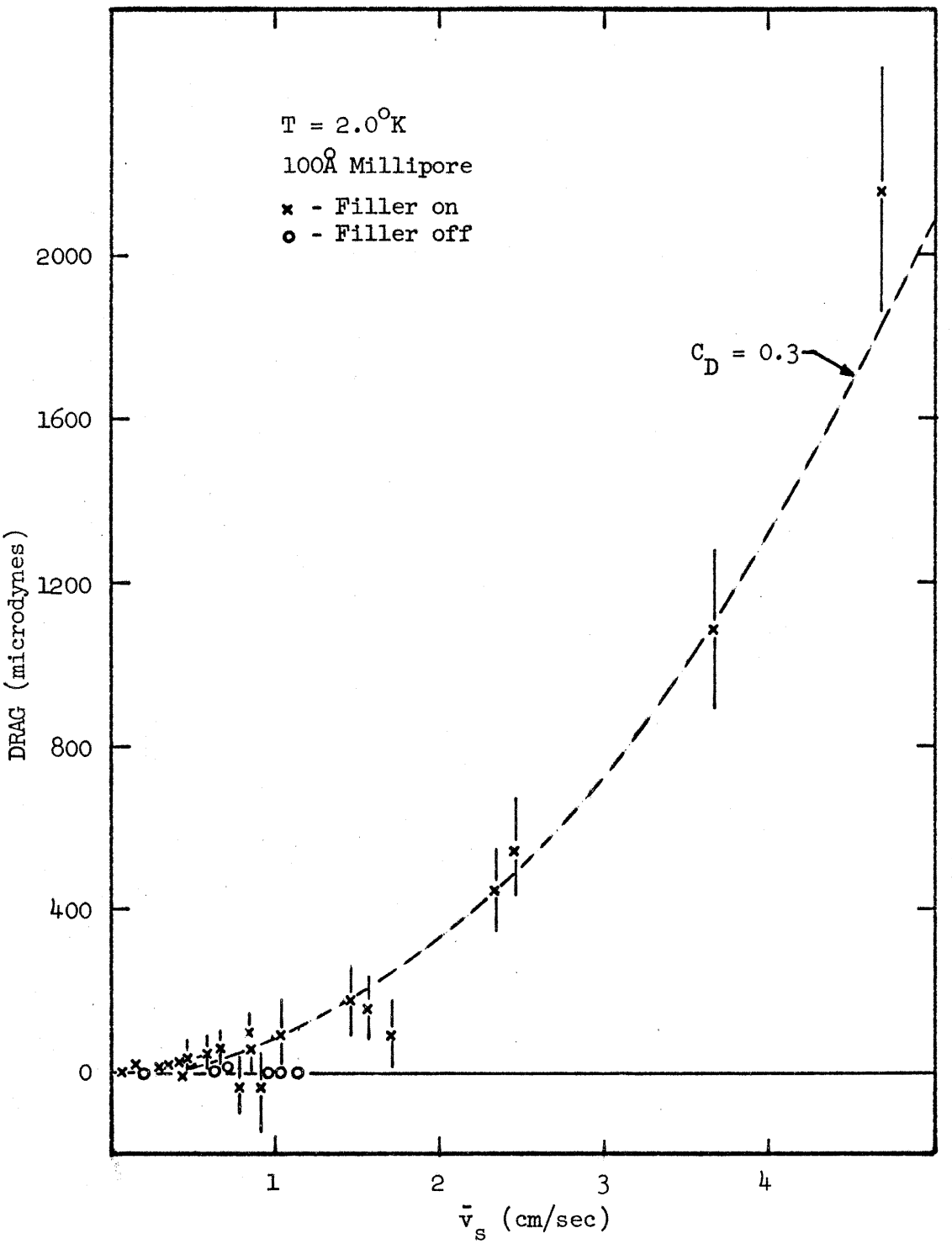


FIGURE 9. Drag on the sphere versus superfluid velocity in the test region, averaged over the cross section. T = 2.0°K.

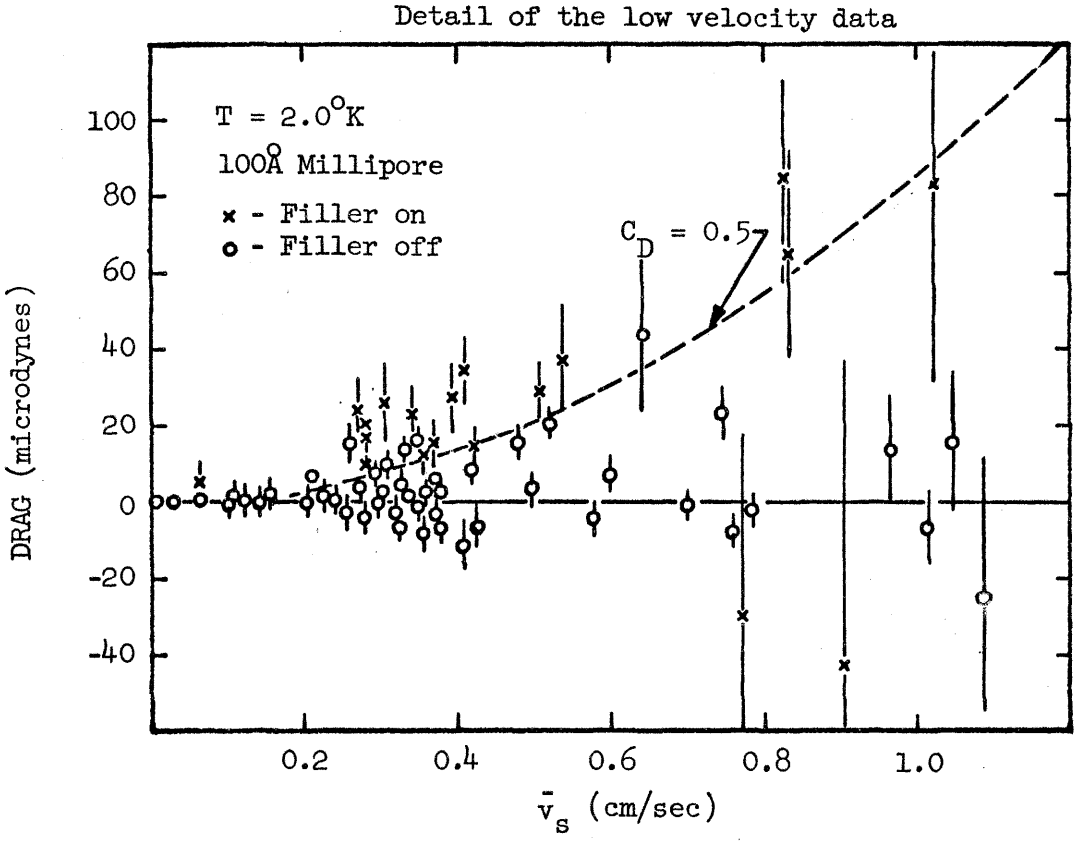


FIGURE 10. Drag on the sphere versus superfluid velocity in the test region, averaged over the cross section (low velocity data on an expanded scale). T = 2.0°K.

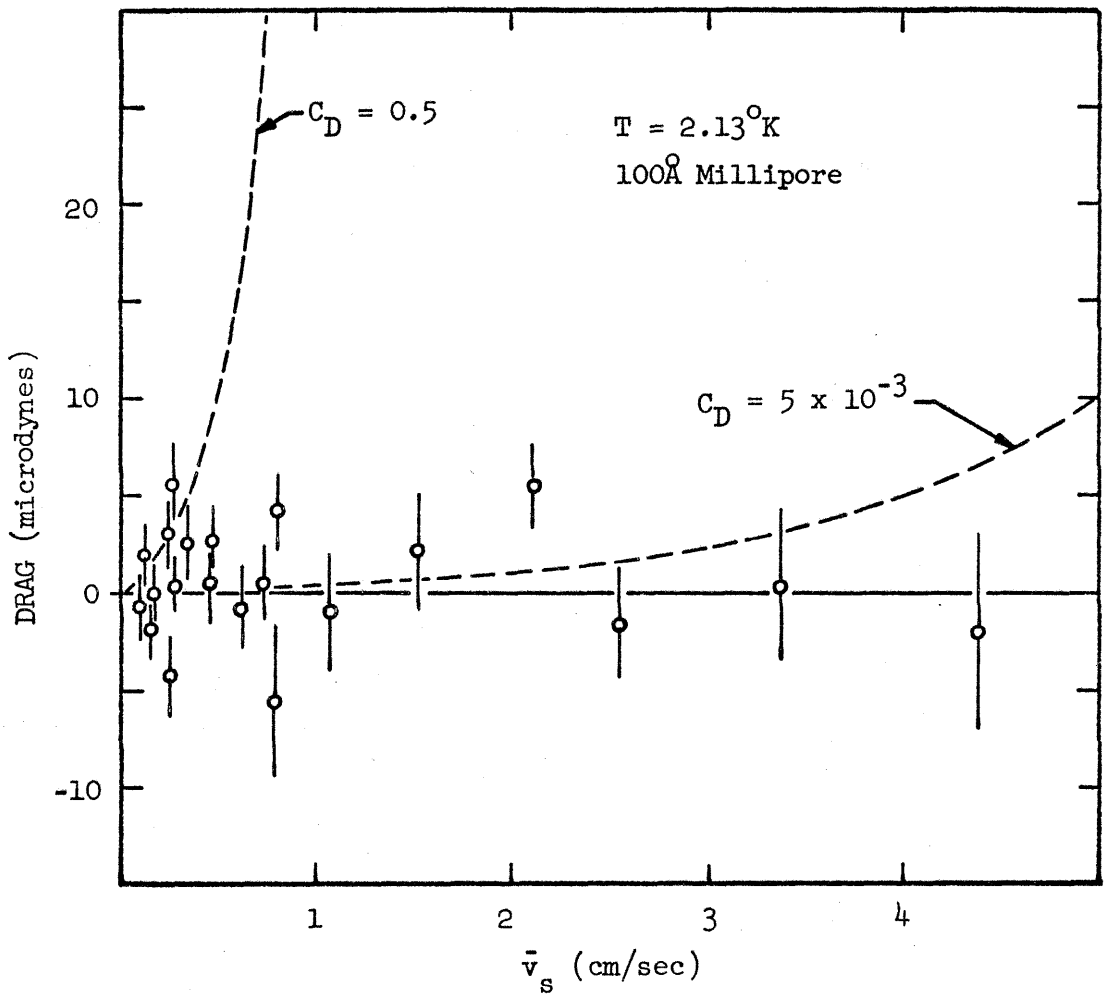


FIGURE 11. Drag on the sphere versus superfluid velocity in the test region, averaged over the cross section. T = 2.13°K.

## 2. Errors

The statistical uncertainty of the data represented in Figures 7 - 11 depends on the uncertainty of both the original measurement and the correction procedure described in Section III-D. Possible errors in both coordinates will be considered.

The superfluid velocity in the test region, $\bar{v}_s$, is calculated from the rate of the change of the helium level in the standpipe, v, and the average velocity of the normal component in the test region, $\bar{v}_n$. The typical statistical error in v is 1 - 2%, with a maximum $\sim$ 3% for very high or low values of v; the error in $\bar{v}_n$ is probably 10%. It should be mentioned that this $\sim$ 10% error in $\bar{v}_n$ represents a major improvement in the accuracy of $\bar{v}_s$ compared to other wind tunnel experiments in which the entire $\bar{v}_n$ term in Equation 6 is neglected.

When numerical values of the actual data are examined, it can be seen that the contribution of the $\bar{v}_n$ term to the value of $\bar{v}_s$ (Equation 6 , page 64 ) usually ranges from a few percent to about half. Then, the total error in $\bar{v}_s$, including errors from both v and $\bar{v}_n$, is usually 3 - 5%. There are a few of the measurements with very small $\bar{v}_s$ in which the major contribution to $\bar{v}_s$ is the $\bar{v}_n$ term, so, for these few points, the uncertainty in $\bar{v}_s$ is as large as 10%.

The drag forces represented by the data in Figures 7 - 11 are limited in accuracy by uncertainties in both the original measurement and in the correction procedure described in Section III-D.

The principal errors in the original measurement are those which come from either the angular resolution of the optical system or the time resolution of the pendulum. For most measure-

ments made at low superfluid velocity, the angular position of the pendulum remained constant within the angular resolution of the optical system about $10^{-3}$ radians. This means that, at low superfluid velocity, the torque on the pendulum, averaged over a time interval comparable to its period, varied less than $10^{-3}$ k' from its long term average. (The effective torsion constant, k', is discussed in Section III-B.) For those values of k' used in this experiment, a torque of $10^{-3}$ k' corresponds to a drag on the sphere and support of 0.4 - 3.1 microdynes. At moderate and high superfluid velocities, the position of the pendulum varied erratically with time, though it remained within fairly well defined limits. The RMS angular deviation from the mean position of the pendulum was calculated for a few measurements from a plot of position versus time, and found to be $\sim$ 75% of the angular distance between the mean position and either limit. It was decided on the basis of this calculation that not enough information was gained to warrant the extra effort required to record the detailed time behavior of the pendulum for each measurement and then calculate the RMS deviation from the mean position, so the limits of motion were taken as the uncertainty in the drag measurement.

The statistical error associated with the correction procedure comes from the measurement of $\Delta h$, and is on the order of 3 - 4% of the correction.

At low superfluid velocities, the resolution of the optical system and the uncertainty in the correction procedure limit the accuracy of the measurement. At moderate and high superfluid velocities, these are unimportant compared to the uncertainty in the estimation of the mean position of the pendulum.

C. "Non-Ideal" Superfluid Flow ($T > 2.14^{\circ}K$)

The data taken at $2.15^{\circ}K$ and $2.163^{\circ}K$ with 100 Å Millipore in the tunnel are shown in Figures 12 and 13. (See Appendix 4 for a table of the original data.) The values of drag have been corrected for the normal component negative drag due to helium head. The superfluid velocity, $\bar{v}_s$, includes the correction for the velocity of the normal component in the test region due to helium head. (The correction procedure is described in Section III-D.) The error bars at moderate and high velocities represent the limits of drag which were observed in any given measurement; at low velocities they represent the statistical error of the correction procedure.

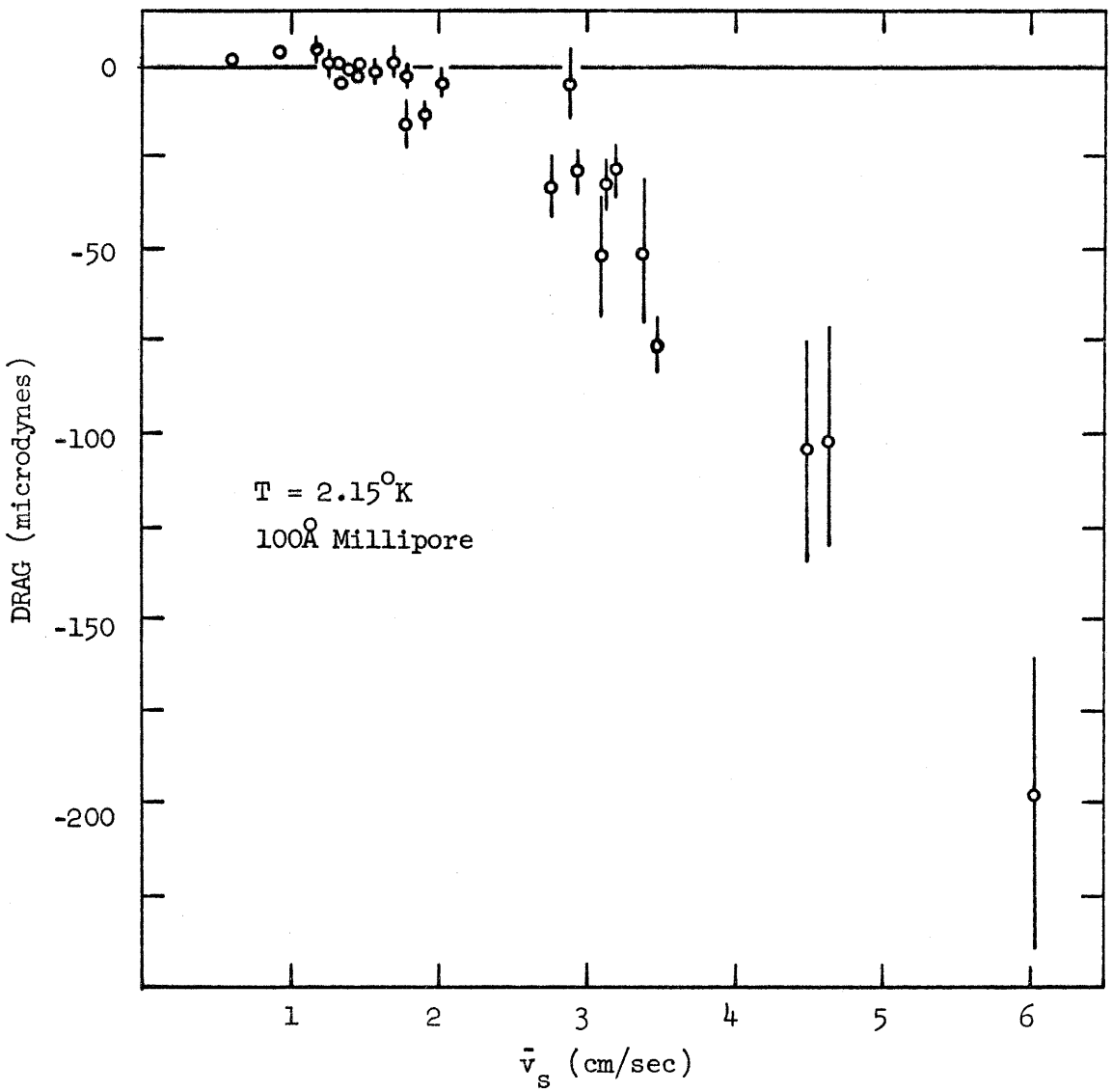


FIGURE 12. Drag on the sphere versus superfluid velocity in the test region, averaged over the cross section (not corrected for the anomalous normal component backflow described in Section V-C). T = 2.15°K.

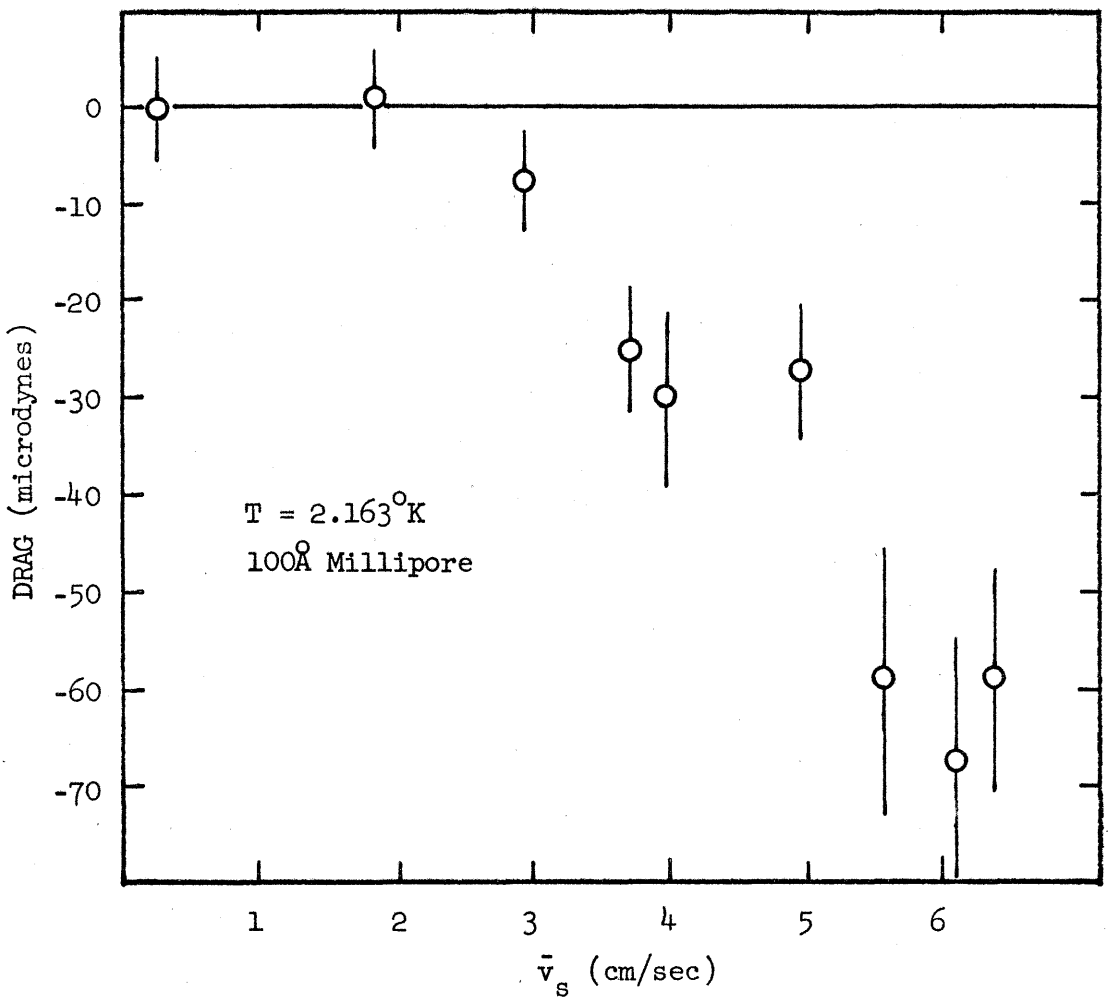


FIGURE 13. Drag on the sphere versus superfluid velocity in the test region, averaged over the cross section (not corrected for the anomalous normal component backflow described in Section V-C). T = 2.163°K.

D. Counterflow

The flow in the test region was intentionally made a counterflow of the superfluid and normal component of helium II at 2.0°K and 2.163°K by putting heat directly into the main chamber. Thus, the superfluid went through the test region from the standpipe to the main chamber, where it was converted to the normal component. Simultaneously, the normal component flowed from the main chamber, through the test region to the standpipe, where it was converted to superfluid by evaporative cooling. The only drag observed at either temperature was in the direction of the flow of the normal component. The results at 2.163°K are shown in Figure 14, where the drag is plotted against both the power put into the main chamber, and against the average normal component velocity in the test region, computed from Equation 10 . The dotted line is a theoretical estimate of the drag on the sphere and support due to the normal component only.

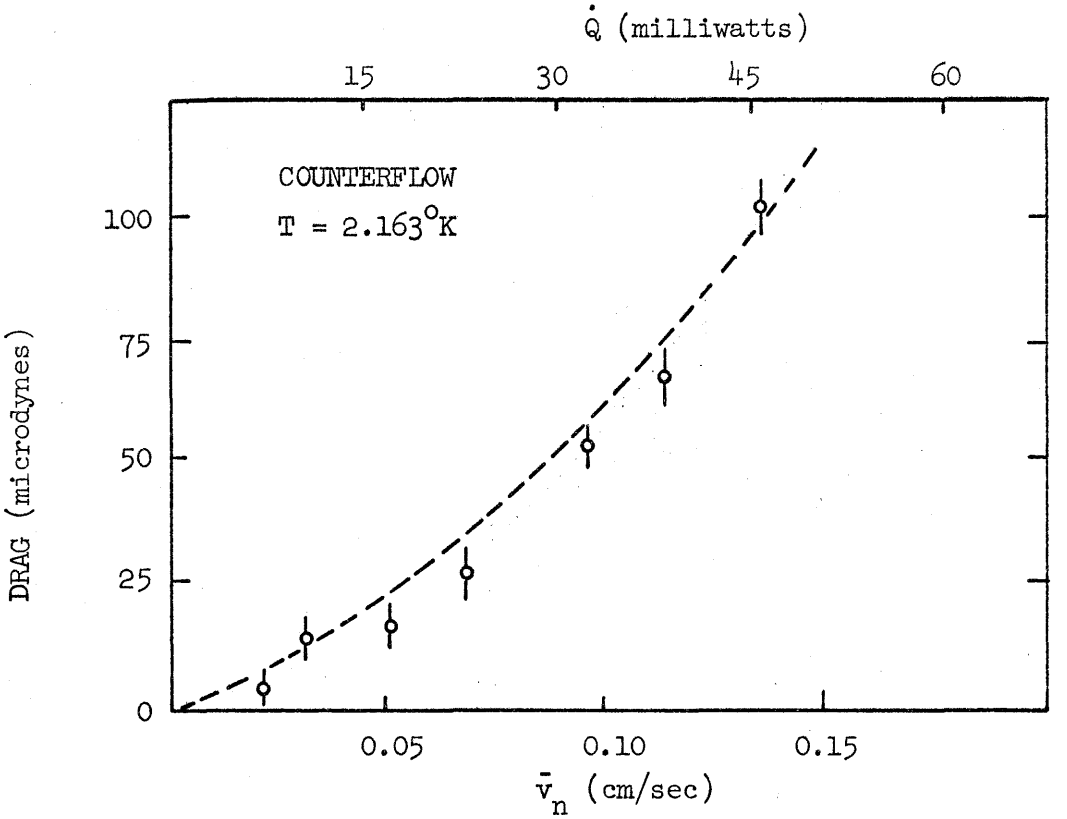


FIGURE 14. Drag on the sphere versus normal component velocity in the test region, averaged over the cross section, and, versus power into main chamber, $\dot{Q}$, in a counterflow of superfluid and normal component. The dotted line is a theoretical estimate of the drag on the sphere and support due to the normal component only.

# V. DISCUSSION

## A. "Ideal" Region of Superfluid Flow ($T < 2.14^{\circ}K$)

### 1. "Filler on" versus "filler off"

The data taken at $1.8^{\circ}K$ with the 500 Å Millipore and that taken at $2.0^{\circ}K$ with 100 Å Millipore each consist of some measurements made with the filler operating continuously and some made 5 - 30 minutes after the filler was turned off. At either temperature, for a given velocity, the measurements made with the filler on almost always gave larger values for the superfluid drag than the measurements made with the filler off. This difference in drag agrees with predictions made from a model of viscosity-free superfluid. If, for example, it is assumed that, at low enough velocity, the superfluid can flow in a non-turbulent, viscosity-free manner, the drag on the sphere will be zero for non-accelerating flows. However, even in a viscosity-free superfluid flow, the drag can be non-zero if turbulence is introduced in the form of vortex lines, and the drag would be expected to increase with the turbulence. Thus, when the filler is running, the helium which hits the splashpan generates turbulence by dripping into the liquid already in the standpipe. This turbulence then flows through the test region with the superfluid and causes drag on the sphere. When the filler is off, however, the superfluid turbulence decays and less drag is observed.

There is, of course, the possibility that the difference in the "filler on" and "filler off" data is related to the action of the filler more directly. This idea was discounted in an early run in which the drag was measured as a function of time after turning off

the filler. The measured drag tended to decrease for the first 3 - 5 minutes and then remain relatively constant. Since the period of the pendulum was only 16 seconds during this run and the temperatures in the helium reestablished equilibrium in the first 30 seconds, it seems clear that the slow decrease in drag was real and represents a decay of turbulence in the helium II rather than some unaccounted for direct action of the filler.

Two questions are immediately suggested on the basis of this model of viscosity-free superfluid with turbulence: Can the superfluid flow be entirely free of turbulence, and, if so, under what conditions and in what velocity region ? Does superfluid flow approach classical behavior under highly turbulent conditions?

These questions will be discussed in the next two sections.

## 2. Turbulent-free Superfluid Flow and Critical Velocities

It can be seen from the data taken below 2.14°K (Figures 7 - 11), that, within experimental error, zero drag was often observed at each temperature. At 1.6°K (Figure 8), zero drag was directly observed up to a superfluid velocity of 0.21 cm/sec and, allowing for somewhat larger errors than shown, there are seven measurements between 0.23 cm/sec and 0.58 cm/sec which might represent zero drag. Similarly, at 1.8°K, zero drag was seen up to $\overline{v}_s$ = 0.48 cm/sec; at 2.0°K, 1.08 cm/sec; and at 2.13°K, 4.4 cm/sec. In fact, at 2.13°K, only zero drag was observed, ± 6

microdynes, for all velocities measured.[22] The temperature variation of the maximum superfluid velocity at which zero drag was observed should not be interpreted as a property of the helium flow. In all cases except 1.6°K it is a direct effect of the instrumentation, in that no higher superfluid velocities were investigated without running the filler and thereby introducing turbulence. The important observation to be made is that, at 1.6°K, 1.8°K, 2.0°K, and 2.13°K, zero drag was often observed in flowing superfluid having free stream velocities up to several centimeters/second. Using the dimensions of the test region, the superfluid critical velocities predicted from the Onsager-Feynman vortex theory are at least 100 times smaller than the largest superfluid velocities at which zero drag was observed. However, these measured velocities are in close agreement with the critical velocities observed by Craig[8], and are the same order of magnitude as those seen by Reppy and Lane[9] and by Bendt[10]. They are also in agreement with the empirical formula reported by

---

(22) At the highest superfluid velocity of 4.4 cm/sec., the theoretical drag on the sphere alone for an ordinary liquid with the velocity and density of the superfluid would be $1.3 \times 10^3$ ($C_D$) microdynes, where $C_D$ is the drag coefficient defined in Appendix 3. Since $C_D$ is always greater than 0.1 for spheres, this theoretical drag would be at least 150 microdynes. The results of the temperature measurements of Section IV-A indicate that, to within the sensitivity of $3 \times 10^{-4}$ degrees, there is no extra temperature drop across the Millipore. Hence, it is believed that this lack of drag at 2.13°K is a property of the superfluid flow, rather than an accidental balance of a large positive superfluid drag and a large normal component negative drag due to something other than the helium head. (The correction due to helium head to the drag represented by the point with $\bar{v}_s = 4.4$ cm/sec was 5 microdynes.)

Van Alphen, Van Haasteren, De Bruyn Ouboter and Taconis.[23] Thus, though the Onsager-Feynman vortex model can be used to describe and predict the qualitative behavior of helium II, it is inadequate as it stands to explain the persistence of dissipation-free superfluid flow in large channels.

### 3. Turbulent Superfluid Flow and the Classical Limit

An examination of the data taken at 1.8°K and 2.0°K shows that most of the "filler on" points, and some of the "filler off" points fall near the parabola calculated from

$$D = C_D (\rho_s \bar{v}_s^2/2) (\pi d^2/4) , \qquad (1)$$

with $C_D = 0.3 - 0.5$, where D is the theoretical drag for a sphere in an infinite fluid with density $\rho_s$ and velocity $\bar{v}_s$, using a drag coefficient of $C_D$. Furthermore, the maximum drag observed at any superfluid velocity at 1.6°K also falls near the same parabola with $C_D \sim 0.7$. Thus, for these three temperatures, the maximum drag due to the superfluid flow is little different from the "classical" drag which would be expected from an ordinary fluid having the density and velocity of the superfluid, if the Reynold's number were greater than about $10^2$, corresponding to an effective viscosity for the "turbulent" superfluid of $10^{-3}$ poise or less (the normal component of helium II has a viscosity $\sim 10^{-5}$ poise). This is in contrast to Craig's experiment in which he reported lift forces in the high velocity limit as small as 0.13 of the classical value. It is possible that a somewhat different mechanism is responsible for

---

(23) W. M. Van Alphen, G. J. Van Haasteren, R. De Bruyn Ouboter and K. W. Taconis, Physics Letters 20, 474 (1966).

superfluid lift than for superfluid drag, and that the force measurements should not be compared. However, it seems more likely that Craig did not take account of the air which was present when he calibrated his system, so he overestimated the sensitivity of his fiber and underestimated the lift which he measured. Since his fractional error would be larger for long periods, sensitive systems, more weight is given to this argument by noting that the discrepancy between Craig's measurements and classical theory was larger for those airfoils for which the expected forces were smaller, and which were presumably measured with more sensitive systems.

In general, the data taken at 1.6°K, 1.8°K, 2.0°K, and 2.13°K are qualitatively consistent with Feynman's theory of quantized vortex lines. Drag is approximately "classical" when the helium II has many vortex lines, as at high velocities or when the helium II has been recently stirred up by the helium II dripping from the comb into the standpipe. At low enough velocities, after the vortices have become microscopic excitations or attached themselves to the walls, the superfluid drag can be zero. Intermediate drag forces are obtained when only a small number of vortex lines are present. (Individual lines would not have been seen in this experiment. The tension in a single vortex line is $\sim 0.1$ microdyne and the greatest sensitivity achieved was $\sim 1/2$ microdyne.)

B. "Non-ideal" Superfluid Flow (> 2.14°K)

The power dependent temperature drop across the 100 Å Millipore which occurs above 2.14°K (see Figure 6) indicates that the helium II can no longer maintain sufficient superfluid flow through the Millipore to keep the exhaust region cool. This is qualitatively in agreement with Seki and Dickson[24] who state that the maximum superfluid flow through 100 Å Millipore decreases rapidly as the transition temperature is reached. If more power is put into the exhaust region than that corresponding to the conversion of the maximum superfluid flow into normal component, the helium II in the exhaust region must become warmer. Eventually, the increased evaporation of helium from the exhaust region, and transport of heat through the Lucite and Millipore from the exhaust region into the bath or main chamber will establish a new steady state with a higher temperature in the exhaust region. The increased evaporation of helium from the exhaust region or the conduction of heat through the Lucite from the exhaust region to the bath have no effect on the flow of helium II through the test region, so do not affect the measurement of drag on the sphere and support or the determination of the superfluid velocity in the test region. However, transport of heat into the main chamber, by any process, significantly affects the flow of helium II through the test region and must be investigated.

An experimental estimate of the minimum velocity of the normal component in the test region which is required to produce the negative 75 microdynes of drag observed at 2.163°K can be

---

(24) H. Seki, C. C. Dickson, Proc. VII Int. Conf. Low Temp. Phys. (edited by Graham and Hollishallet), p. 569 (University of Toronto Press, 1961).

obtained from the results of Section IV-D, where heat was put directly into the main chamber to produce a flow of superfluid through the test region into the main chamber and a counterflow of normal component from the main chamber into the test region. A negative drag of 75 microdynes was measured in this counterflow at 2.163°K when the power input to the main chamber was 40 milliwatts (see Figure 14). This 40 milliwatts will produce an average normal fluid velocity in the test region, $\bar{v}_n$, of 0.12 cm/sec (Equation 10 ). (The theoretical estimate of the drag on the sphere and support due to the normal component at 2.163°K flowing with a velocity of 0.12 cm/sec, is 72 microdynes.)

It would seem, then, that the negative drag of 75 microdynes observed at 2.163°K when the tunnel was being run as a "superfluid wind tunnel" (Figure 13) is caused by a normal component flow opposite to the superfluid flow having an average velocity of 0.12 cm/sec in the test region. I cannot explain how enough heat or normal fluid gets into the main chamber from the exhaust region to produce this much normal component flow. At the observed temperature difference across the Millipore of $9 \times 10^{-3}$ degrees, the conduction of heat from the exhaust region through the Millipore into the main chamber can be calculated to be one milliwatt, assuming a thermal conductivity of $6 \times 10^{-4}$ watt $cm^{-1}$ $degree^{-1}$ for the cellulose esters composing the web of the Millipore. One milliwatt would produce an average normal component velocity in the test region of only $3 \times 10^{-3}$ cm/sec.

There should also be a direct flow of normal component from the exhaust region through the pores of the Millipore due to the temperature drop across the Millipore. This can be crudely estimated by looking at the coefficients of the hydrodynamic equation of motion for the normal component,

$$\rho_n \frac{D\bar{v}_n}{Dt} = -\frac{\rho_n}{\rho} \nabla P - \rho_s S \nabla T + \eta_n \left( \nabla^2 v_n + \frac{1}{3} \nabla\nabla \cdot v_n \right). \qquad (2)$$

A temperature difference, $\Delta T$, contributes the same acceleration to the normal component as a pressure difference of $(\rho_s/\rho_n)$ $(\rho S \Delta T)$. Then, a $\Delta T$ of $9 \times 10^{-3}$ degrees at $2.163^{\circ}K$, corresponds to a 3 cm head of liquid helium, which according to the correction procedure used in Section III-D, corresponds to $\bar{v}_n = 15 \times 10^{-3}$ cm/sec. Thus, the total normal component flow in the test region at $2.163^{\circ}K$ due to a $9 \times 10^{-3}$ degree temperature drop across the Millipore is theoretically estimated to be $18 \times 10^{-3}$ cm/sec, which is only 15% of the value obtained from the counter-flow experiment.

Since the observed drag is that due to the superfluid minus that of the normal component, and there is no independent estimate of either one alone, the effects cannot be separated in the high temperature "non-ideal" operation ($> 2.14^{\circ}K$).

# VI. CONCLUSIONS

A "superfluid wind tunnel" was developed which has a much steadier superfluid flow than similar tunnels used in previous work. With this improved tunnel, the investigation of the drag on a sphere in a predominately superfluid flow was carried out with about ten times the torque sensitivity of other superfluid wind tunnel experiments and, at the same time, the heavy damping to the measuring system which was necessary in those experiments could be eliminated. Thus, small forces due to the flowing helium could be observed with a time constant of 10 - 15 seconds; larger forces could be observed on an even shorter time scale.

At 1.6°K, 1.8°K and 2.0°K, the maximum drag observed for a given superfluid velocity corresponded to a drag coefficient of 0.7 at 1.6°K, 0.5 at 1.8°K and 0.3 at 2.0°K ($\pm$ 20%). This is comparable to that which would be produced by an ordinary, low viscosity liquid (defined as having the density and velocity of the superfluid), and should be contrasted to the results reported by Craig, which indicated that the lift on an airfoil due to rapidly flowing superfluid is only 0.13 to 0.55 of the lift expected from an ordinary, viscous liquid. While it is possible that different mechanisms for producing the forces are involved in the two experiments, and the results are actually consistent with each other, it is believed instead that the relatively low forces reported by Craig are due to a calibration error on his part.

Within the experimental error, zero drag was often observed for superfluid velocities up to 0.21 cm/sec at 1.6°K, 0.48 cm/sec at 1.8°K, 1.1 cm/sec at 2.0°K and 4.4 cm/sec at 2.13°K. (These velocities are not necessarily critical velocities, but are probably

limits imposed by the measurement technique. They are, however, minimum values of the superfluid critical velocity at each temperature.) These velocities are much higher than the critical velocities predicted from the Onsager-Feynman model of quantized vortex lines, but are in good agreement with those measured in other large dimension superfluid flow experiments.

At 2.13$^{o}$K, only zero drag was observed up to the maximum superfluid velocity measured (4.4 cm/sec). (Even allowing for the experimental error, this corresponds to a maximum drag coefficient of only $4 \times 10^{-3}$.) At the other three temperatures, however, steady, non-zero values of drag which were less than the maximum drag obtained at other times under essentially the same experimental conditions were also observed. This result is qualitatively consistent with the quantized vortex model. Thus, it seems that the vortex line model furnishes plausible explanations of experimental observations, but fails to yield quantitatively correct predictions.

## APPENDIX 1 - Determination of the Superfluid Velocity

A. Definition of symbols:

$\rho$ = mass density of helium II.

$\rho_n$ = mass density of normal component of helium II.

$\rho_s$ = mass density of superfluid component of helium II.

$\bar{v}_s$ = superfluid velocity in the test region, averaged over the cross section. Positive direction is from the test region to the exhaust.

$\bar{v}_n$ = normal component velocity in the test region, averaged over the cross section. Positive direction is opposite to that of $\bar{v}_s$.

$v_n$ = effective normal component velocity in the vicinity of the sphere and support. Positive direction is opposite to that of $\bar{v}_s$.

$v$ = rate of change of level of helium II in standpipe. Positive direction is downward.

$\dot{z}$ = rate of helium II evaporation from standpipe, (mass per unit time).

$S$ = entropy / unit mass of helium II.

$S_n$ = entropy / unit mass of the normal component.

$L$ = latent heat of evaporation / unit mass of helium II.

$A$ = cross sectional area of standpipe.

$a$ = cross sectional area of test region.

B. Calculation

With the tunnel running normally, superfluid will go through the Millipore into the exhaust region of the tunnel, some of the normal component will leak back, helium II will evaporate from both sides of the tunnel, the level in the standpipe will go down and helium II will pour into the bath from the exhaust. The largest temperature difference observed in this experiment was $9 \times 10^{-3}$ degrees between the exhaust region and the main bath. Even at this maximum, the heat conduction through the Lucite or Millipore is negligible for the purposes of this experiment and will be neglected in all calculations.

Then, the total rate of helium loss in the standpipe region is

$$-\rho v A = -\rho_s \bar{v}_s a + \rho_n \bar{v}_n a - \dot{z}. \tag{3}$$

Similarly, remembering that the superfluid carries no entropy, the entropy loss from the standpipe is

$$-\rho v A S = \rho_n \bar{v}_n a S_n - \dot{z}\ (S + L/T). \tag{4}$$

We can compute $S_n$ by the relation

$$\rho S = \rho_n S_n. \tag{5}$$

Then, eliminating $\dot{z}$, and solving for $\bar{v}_s$, we get

$$\bar{v}_s = (\rho/\rho_s)(A/a)[1 - ST/(L + ST)]v + (\rho/\rho_s)[\rho_n/\rho - ST/(L + ST)]\bar{v}_n . \tag{6}$$

If the tunnel is perfect, i. e., there is no back flow of the normal component, then

$$\bar{v}_s = (\rho/\rho_s)(A/a)[1 - ST/(L + ST)]v . \tag{7}$$

All the thermodynamic functions in this equation are tabulated, A and a are geometrical constants of the wind tunnel and v is directly observed during a run.

In general, however, there is a backflow of normal component, so $\bar{v}_n$ is not zero and it must be estimated. In the present investigation, the adjusted values of $\bar{v}_n$ discussed in Section III-D-2 were used in Equation 6 to calculate $\bar{v}_s$.

The equation for $\bar{v}_s$ takes on a much simpler form when describing counterflow. Then, conservation of mass requires that

$$\rho v A = \dot{z} \; ; \; \rho_s \bar{v}_s = \rho_n \bar{v}_n . \tag{8}$$

This gives

$$\bar{v}_s = (\rho_n/\rho_s)(A/a)(L/ST)v . \tag{9}$$

If $(\dot{Q}/a)$ is the rate of heat flow per unit cross sectional area in the test region, then

$$(\dot{Q}/a) = \rho \bar{v}_n ST , \tag{10}$$

and

$$\bar{v}_s = \bar{v}_n(\rho_n/\rho_s) = (\rho_n/\rho_s)(\dot{Q}/a)(1/\rho ST) \quad . \tag{11}$$

## APPENDIX 2 - Measurement of Temperature Differentials With Carbon Resistors

An easy and accurate method of determining small temperature differences in helium II is by monitoring the resistance of carbon resistors. Ohmite "Little Devil" 1/10 watt 5% 22 ohm resistors were incorporated into the "superfluid wind tunnel". Their resistance was measured versus temperature with a General Radio Impedance Bridge, Type 1650A, and dR/dT was calculated as a function of temperature from this data. For any given temperature, dR/dT had the same value on different runs to within 1%.

The circuit shown in Figure 15 was used to measure small changes in resistance of any of the temperature sensing resistors. The CRL potentiometer of the General Radio Bridge was set on a value of resistance near to, but higher than, the resistor being measured. The decade box and Helipot in series with the resistor were adjusted for the best null on the General Radio Null Detector. (Usually, some capacitance had to be added in parallel with the resistors in order to get a good null.) When the temperature sensing resistor changed its resistance, the decade box and Helipot were readjusted to bring the bridge back to null. The change in their resistance is the change of the temperature sensing resistor, with the opposite sign. Then, the temperature difference can be obtained from $\Delta T = (dR/dT)^{-1} \Delta R$.

In the present experiment, the temperature sensitivity achieved was $3 \times 10^{-4}$ degrees at $2^{o}K$.

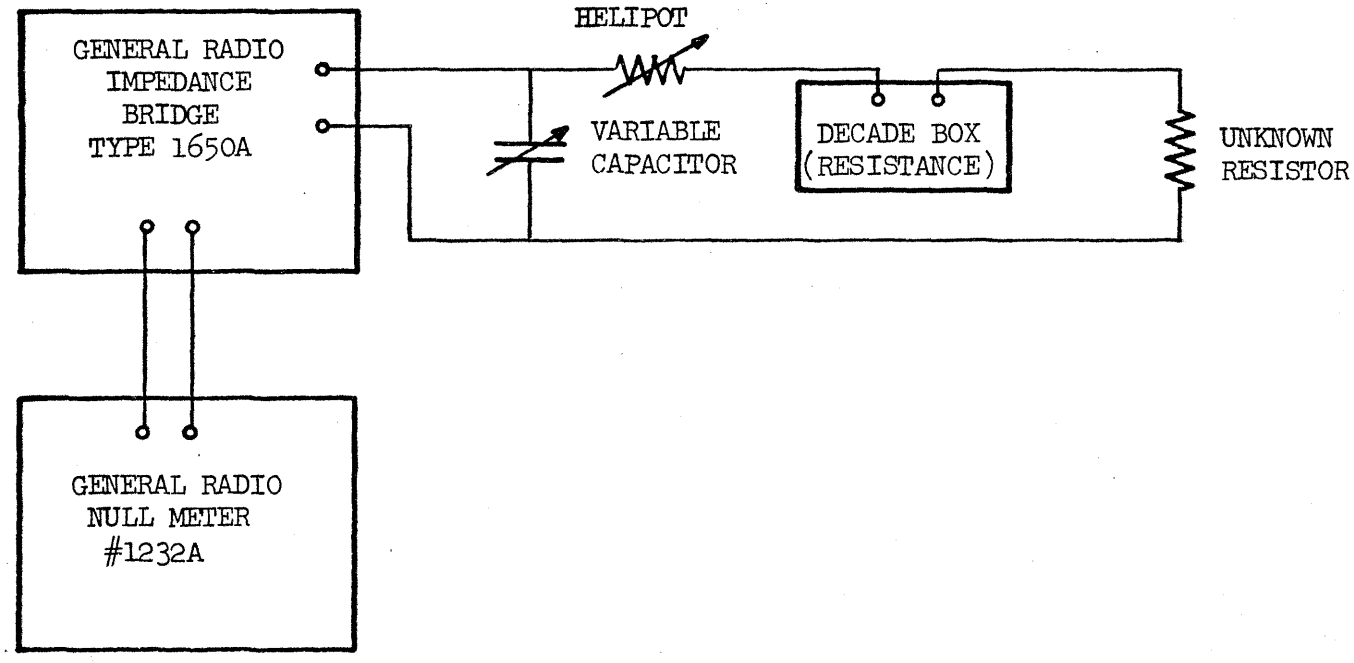


FIGURE 15. Schematic diagram of circuit used to measure small changes in resistance.

## APPENDIX 3 - Drag on a Sphere

The special case of drag on a sphere in a non-accelerating flow of an ordinary viscous liquid at subsonic velocities is readily described in terms of a dimensionless parameter, the Reynolds number. This is a measure of the ratio of inertial to viscous forces, and is defined by

$$R = \rho v d/\eta \quad , \tag{12}$$

where $\rho$ is the density of the fluid; v, the free stream velocity; d, the diameter of the sphere; $\eta$, the viscosity of the fluid.

It is convenient to define another dimensionless parameter, the drag coefficient, $C_D$, by the relation

$$D = C_D \, (\rho v^2/2) \, A \quad , \tag{13}$$

where D is the drag force and A the projected area of the test object. An experimental plot of $C_D$ versus R is shown in Figure 16 from which it can be seen that $C_D$ is uniquely determined for all conditions having the same R.

For $R < 1$, the flow is strongly dominated by viscous effects and the drag on a sphere can be calculated from Stokes law,

$$D = 3\pi\eta v d \, , \tag{14}$$

which makes $C_D$ inversely proportional to R.

Inertial effects contribute to the drag for $R > 1$. By the time a Reynolds number of 10 is reached, the flow has

separated near the equator and there is a steady vortex system behind the sphere. At higher Reynolds numbers, vortices separate from the sphere in a fairly irregular manner.

At a critical Reynolds number around $3 \times 10^5$, the pattern of flow around the sphere changes again and the drag coefficient decreases rapidly to about 1/4 of the value it had at lower Reynolds numbers.

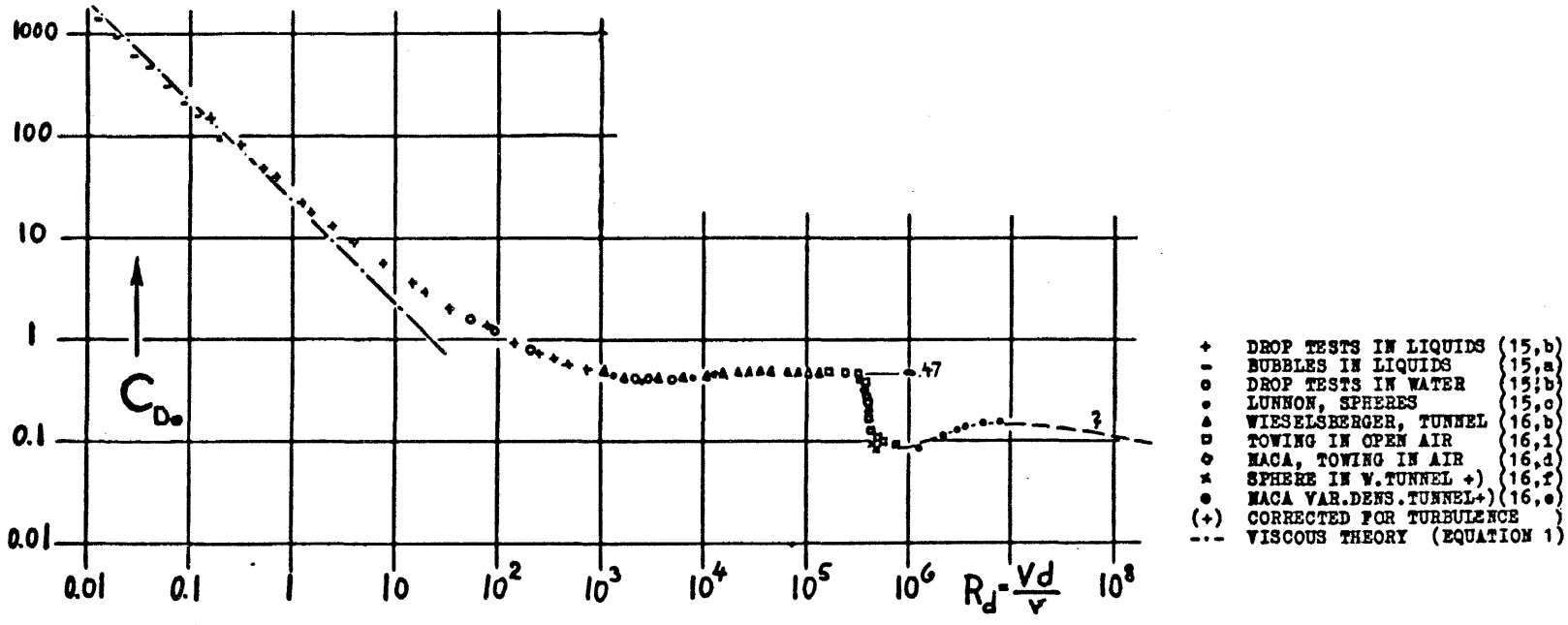


FIGURE 16. Experimental drag coefficients of the sphere as a function of Reynolds number. (Reprinted from Hoerner, Fluid Dynamic Drag.)

# APPENDIX 4 - Data

The tables on the following pages contain the original data, the corrections to the original data (calculated according to the procedure described in Section III-D), and the corrected data (plotted in Figures 7 - 13). The data are listed by the date of the run and in the order they were taken during that run. The column headings mean the following:

$D$ = drag on the sphere (microdynes). The direction of the superfluid flow is positive.

$\Delta h$ = difference in height between the surface of the liquid helium in the exhaust and in the standpipe (cm).

$v$ = rate of change of the helium level in the standpipe at the time $D$ was measured ($10^{-3}$ cm/sec).

$\Delta$ = correction to be added to the measured drag, (according to the procedure described in Section III-D) (microdynes).

$D + \Delta$ = corrected drag (microdynes).

$\overline{v}_s$ = superfluid velocity in the test region, averaged over the cross section cm/sec.

$\pm$ = estimate of error in $D + \Delta$ (microdynes).

## 1.6°K Data

### 6 March 1966

| D | Δh | v | Δ | D + Δ | $\bar{v}_s$ | ± | Filler |
|---|---|---|---|---|---|---|---|
| 4 | 5.1 | 8.6 | 5 | 1 | 0.054 | 2 | No |
| - 2 1/2 | 9.2 | 23.5 | 9 1/2 | 7 | 0.136 | 2 | No |
| - 8 1/2 | 16.0 | 76 | 18 1/2 | 10 | 0.40 | 4 | No |
| 84 | 2.5 | 181 | 2 1/2 | 86 | 0.88 | 15 | No |
| 71 | 6.1 | 148 | 6 | 77 | 0.73 | 14 | No |
| 51 | 9.0 | 108 | 9 | 60 | 0.54 | 9 | No |
| 54 | 12.2 | 87 | 13 | 67 | 0.45 | 6 | No |
| 29 | 14.5 | 76 | 16 1/2 | 46 | 0.40 | 5 | No |
| 16 | 16.2 | 66 | 18 1/2 | 34 | 0.35 | 3 | No |
| - 7 | 8.4 | 7.7 | 8 1/2 | 1 1/2 | 0.058 | 2 | No |
| 139 | 2.0 | 120 | 2 | 141 | 0.58 | 20 | No |
| 2 1/2 | 11.5 | 110 | 12 1/2 | 15 | 0.59 | 5 | No |

### 7 March 1966

| | | | | | | | |
|---|---|---|---|---|---|---|---|
| - 2 | 2.0 | 1.4 | 2 | 0 | 0.011 | 2 | No |
| 14 1/2 | 4.5 | 59 | 4 1/2 | 19 | 0.29 | 3 | No |
| 13 | 7.5 | 38 | 8 | 21 | 0.201 | 3 | No |
| - 7 1/2 | 10.0 | 17.3 | 10 1/2 | 3 | 0.108 | 3 | No |
| -12 | 11.0 | 10.1 | 11 1/2 | - 1/2 | 0.076 | 3 | No |
| 42 | 2.0 | 90 | 2 | 44 | 0.43 | 5 | No |
| - 7 | 13.6 | 26 | 15 | 8 | 0.160 | 4 | No |
| -17 | 16.0 | 9.6 | 19 | 2 | 0.086 | 3 | No |
| - 1 | 1.0 | 2.7 | 1 | 0 | 0.019 | 2 | No |

## 1.6°K Data (cont.)

| D | Δh | v | Δ | D + Δ | $\bar{v}_s$ | ± | Filler |
|---|---|---|---|---|---|---|---|
| -11 | 8.9 | 2.6 | 9 | - 2 | 0.035 | 2 | No |
| 70 | 2.0 | 70 | 2 | 72 | 0.34 | 10 | No |
| 18 | 5.0 | 59 | 5 | 23 | 0.29 | 5 | No |
| 11 1/2 | 7.0 | 43 | 7 | 18 1/2 | 0.224 | 2 | No |
| - 9 | 9.2 | 29 | 9 1/2 | 1/2 | 0.165 | 2 | No |
| -12 | 10.6 | 22.2 | 11 | - 1 | 0.133 | 2 | No |
| 84 | 2.0 | 100 | 2 | 86 | 0.48 | 8 | No |
| 6 | 5.0 | 74 | 5 | 11 | 0.37 | 3 | No |
| 0 | 8.5 | 57 | 8 1/2 | 8 1/2 | 0.30 | 2 | No |
| -12 1/2 | 11.2 | 40 | 12 | - 1/2 | 0.207 | 3 | No |
| -14 1/2 | 11.5 | 4.0 | 12 1/2 | - 2 | 0.047 | 3 | No |
| 98 | 2.0 | 120 | 2 | 100 | 0.58 | 12 | No |
| 0 | 8.0 | 53 | 8 | 8 | 0.27 | 2 | No |
| 15 | 10.3 | 48 | 11 | 26 | 0.252 | 3 | No |
| -12 | 12.8 | 36 | 14 | 2 | 0.207 | 2 | No |
| 113 | 4.5 | 98 | 4 1/2 | 118 | 0.48 | 22 | No |
| 29 | 9.3 | 72 | 9 1/2 | 38 | 0.36 | 5 | No |
| 57 | 12.2 | 56 | 13 1/2 | 70 | 0.30 | 8 | No |
| 15 1/2 | 14.2 | 46 | 16 | 32 | 0.25 | 6 | No |
| 58 | 2.0 | 120 | 2 | 60 | 0.58 | 7 | No |
| 55 | 5.0 | 110 | 5 | 60 | 0.53 | 10 | No |
| 85 | 7.5 | 88 | 7 1/2 | 92 | 0.44 | 8 | No |
| 83 | 9.0 | 74 | 9 | 92 | 0.37 | 14 | No |
| 1 | 11.5 | 67 | 12 1/2 | 13 1/2 | 0.35 | 3 | No |
| 30 | 13.0 | 57 | 14 1/2 | 45 | 0.30 | 6 | No |
| 140 | 2.0 | 140 | 2 | 142 | 0.67 | 20 | No |

## 1.6°K Data (cont.)

| D | Δh | v | Δ | D + Δ | $\bar{v}_s$ | ± | Filler |
|---|---|---|---|---|---|---|---|
| 34 | 8.0 | 97 | 8 | 42 | 0.49 | 4 | No |
| 60 | 11.0 | 75 | 12 | 72 | 0.39 | 6 | No |
| - 9 | 15.0 | 46 | 17 | 8 | 0.26 | 3 | No |
| 225 | 20 | 204 | 2 | 227 | 0.96 | 40 | No |
| 195 | 5.0 | 145 | 5 | 200 | 0.72 | 30 | No |
| 170 | 8.0 | 140 | 8 | 178 | 0.69 | 25 | No |
| 115 | 11.4 | 125 | 12 1/2 | 128 | 0.65 | 18 | No |

## 1.8°K Data

### 22 December 1965

| D | Δh | v | Δ | D + Δ | $\bar{v}_s$ | ± | Filler |
|---|---|---|---|---|---|---|---|
| - 2 | 0.8 | 3.2 | 2 | 0 | 0.034 | 2 | Yes |
| - 21 | 3.2 | 15.1 | 29 | 8 | 0.150 | 4 | Yes |
| 16 | 4.1 | 131 | 40 | 56 | 0.83 | 8 | Yes |
| 2040 | 2.0 | 500 | 12 | 2052 | 2.89 | 350 | Yes |
| - 46 | 5.4 | 22.2 | 78 | 32 | 0.235 | 10 | Yes |

### 23 December 1965

| | | | | | | | |
|---|---|---|---|---|---|---|---|
| - 10 | 1.5 | 0.9 | 8 | - 2 | 0.035 | 3 | Yes |
| - 7 | 1.5 | 12.0 | 8 | 1 | 0.098 | 3 | Yes |
| 6 | 1.0 | 33 | 5 | 11 | 0.208 | 2 | Yes |
| 23 | 0.7 | 50 | 3 | 26 | 0.30 | 5 | Yes |
| - 8 | 2.0 | 59 | 11 | 3 | 0.38 | 3 | Yes |
| - 5 | 1.4 | 2.3 | 8 | 3 | 0.041 | 2 | Yes |

### 24 December 1965

| | | | | | | | |
|---|---|---|---|---|---|---|---|
| - 3 | 0.5 | 3.1 | 1 | - 2 | 0.028 | 2 | Yes |
| - 3 | 1.0 | 3.0 | 5 | 2 | 0.037 | 3 | Yes |
| - 9 | 2.0 | 6.4 | 12 | 3 | 0.076 | 4 | Yes |
| - 3 | 1.1 | 25 | 5 | 2 | 0.164 | 3 | Yes |
| 13 | 1.0 | 38 | 5 | 18 | 0.237 | 4 | Yes |
| - 4 | 1.1 | 2.7 | 5 | 1 | 0.037 | 2 | Yes |

## 1.8°K Data (cont.)

25 December 1965

| D | Δh | v | Δ | D + Δ | $\bar{v}_s$ | ± | Filler |
|---|---|---|---|---|---|---|---|
| - 19 | 2.5 | 23.5 | +16 | - 3 | 0.184 | 5 | Yes |
| - 11 | 1.6 | 15.2 | 9 | - 2 | 0.119 | 3 | Yes |
| 0 | 0.8 | 9.8 | 2 | 2 | 0.072 | 2 | Yes |
| - 11 | 2.3 | 1.2 | 14 | 3 | 0.053 | 3 | No |
| - 18 | 2.7 | 27 | 20 | 2 | 0.208 | 4 | Yes |
| 53 | 1.7 | 43 | 9 | 62 | 0.279 | 9 | Yes |
| 73 | 2.3 | 80 | 15 | 88 | 0.50 | 12 | Yes |
| 164 | 1.0 | 151 | 6 | 170 | 0.88 | 60 | Yes |
| 330 | 2.4 | 210 | 15 | 345 | 1.25 | 80 | Yes |

26 December 1965

| | | | | | | | |
|---|---|---|---|---|---|---|---|
| 4 | 3.1 | 68 | 24 | 28 | 0.45 | 7 | Yes |
| 80 | 2.4 | 110 | 15 | 95 | 0.68 | 15 | Yes |
| 217 | 5.2 | 169 | 69 | 286 | 1.07 | 150 | Yes |
| 700 | 2.1 | 240 | 14 | 714 | 1.41 | 200 | Yes |
| 1020 | 0.9 | 295 | 3 | 1023 | 1.70 | 200 | Yes |

30 December 1965

| | | | | | | | |
|---|---|---|---|---|---|---|---|
| 0 | 0.6 | 1.0 | 1 | 1 | 0.018 | 1 | No |
| - 8 | 2.0 | 2.1 | 11 | 3 | 0.052 | 2 | No |
| - 27 | 3.5 | 2.9 | 29 | 2 | 0.087 | 6 | No |
| - 29 | 3.5 | 5.2 | 29 | 0 | 0.100 | 6 | No |

## 1.8°K Data (cont.)

30 December 1965 (cont.)

| D | Δh | v | Δ | D + Δ | $\bar{v}_s$ | ± | Filler |
|---|---|---|---|---|---|---|---|
| 0 | 0.4 | 2.0 | 1 | 1 | 0.019 | 1 | No |
| - 3 | 0.6 | 0.9 | 2 | - 1 | 0.017 | 1 | No |

4 January 1966

| | | | | | | | |
|---|---|---|---|---|---|---|---|
| - 3 | 1.2 | 19.4 | 5 | 2 | 0.135 | 2 | No |
| - 10 | 1.8 | 9.3 | 9 | - 1 | 0.089 | 2 | No |
| - 16 | 2.2 | 4.6 | 16 | 0 | 0.070 | 3 | No |
| - 16 | 2.5 | 43 | 18 | 2 | 0.295 | 3 | No |
| - 21 | 2.8 | 4.0 | 23 | 2 | 0.079 | 4 | No |
| - 30 | 3.8 | 32 | 35 | 5 | 0.26 | 4 | No |
| - 17 | 3.2 | 46 | 26 | 9 | 0.326 | 4 | No |
| - 50 | 4.4 | 14.1 | 48 | - 2 | 0.168 | 6 | No |
| - 18 | 2.5 | 3.9 | 18 | 0 | 0.072 | 3 | No |
| - 70 | 5.4 | 24 | 73 | 3 | 0.245 | 6 | No |
| - 72 | 5.6 | 5.1 | 75 | 3 | 0.141 | 6 | No |
| - 76 | 5.7 | 6.0 | 77 | 1 | 0.148 | 6 | No |
| - 80 | 5.7 | 5.9 | 77 | - 3 | 0.148 | 6 | No |
| - 119 | 6.9 | 12.9 | 115 | - 4 | 0.212 | 8 | No |
| - 57 | 4.9 | 70 | 56 | 1 | 0.50 | 5 | No |

## 2.0°K Data

### 15 February 1966

| D | Δh | v | Δ | D + Δ | $\bar{v}_s$ | ± | Filler |
|---|---|---|---|---|---|---|---|
| -12 1/2 | 6.5 | 26 | 9 | -3 1/2 | 0.37 | 3 | No |
| - 8 | 8.0 | 18.8 | 11 | 3 | 0.33 | 3 | No |
| -14 | 9.4 | 11.9 | 13 | -1 | 0.29 | 3 | No |
| -19 | 10.8 | 8.2 | 15 1/2 | -3 1/2 | 0.28 | 4 | No |
| -20 | 11.9 | 4.0 | 17 1/2 | -2 1/2 | 0.26 | 4 | No |
| 11 1/2 | 10.9 | 11.2 | 15 1/2 | 27 | 0.31 | 12 | Yes |
| 5 | 13.0 | 3.8 | 19 | 24 | 0.27 | 10 | Yes |
| -14 | 11.2 | 2.8 | 16 | 2 | 0.23 | 3 | No |
| - 9 1/2 | 7.2 | 7.5 | 10 | 1/2 | 0.205 | 4 | No |

### 16 February 1966

| | | | | | | | |
|---|---|---|---|---|---|---|---|
| 2 | 1.0 | 5.0 | 1 | 3 | 0.068 | 3 | Yes |
| - 1/2 | 1.4 | 4.0 | 1 1/2 | 1 | 0.065 | 2 | No |
| -14 1/2 | 12.0 | 15.0 | 17 1/2 | 3 | 0.37 | 3 | No |
| -15 | 13.1 | 8.8 | 19 | 4 | 0.32 | 3 | No |
| -16 | 15.5 | 1.7 | 24 | 8 | 0.30 | 3 | No |
| 23 | 3.5 | 45 | 4 1/2 | 28 | 0.51 | 10 | Yes |
| 5 1/2 | 5.7 | 32 | 7 1/2 | 13 | 0.42 | 8 | Yes |
| - 1/2 | 7.8 | 28 | 10 1/2 | 10 | 0.42 | 2 | No |
| - 6.5 | 10.5 | 18.8 | 14 1/2 | 8 | 0.38 | 2 | No |
| - 4 | 13.0 | 10.8 | 19 | 15 | 0.34 | 4 | No |
| -12 | 15.0 | 0.9 | 23 | 11 | 0.28 | 3 | No |
| -12 | 10.6 | 10.6 | 15 | 3 | 0.30 | 4 | No |

## 2.0°K Data (cont.)

16 February 1966 (cont.)

| D | Δh | v | Δ | D + Δ | $\bar{v}_s$ | ± | Filler |
|---|---|---|---|---|---|---|---|
| -16 | 15.9 | 0.2 | 25 | 9 | 0.29 | 5 | Yes |
| - 3 | 10.8 | 16.2 | 15 1/2 | 12 | 0.36 | 5 | Yes |
| 14 1/2 | 9.0 | 24 | 12 1/2 | 27 | 0.40 | 10 | Yes |
| 22 1/2 | 8.3 | 27 | 11 | 34 | 0.42 | 10 | Yes |
| -24 | 9.4 | 24 | 13 | -11 | 0.41 | 5 | Yes |
| 1/2 | 11.0 | 17.2 | 15 1/2 | 16 | 0.37 | 6 | Yes |
| - 1/2 | 14.5 | 8.1 | 22 | 22 | 0.34 | 8 | Yes |
| -12 | 11.4 | 9.0 | 16 | 4 | 0.30 | 2 | No |
| -12 1/2 | 8.1 | 5.3 | 11 | - 1 1/2 | 0.197 | 4 | No |
| - 5 | 6.0 | 26.7 | 8 | 3 | 0.38 | 4 | No |
| 1/2 | 10.3 | 15.1 | 14 | 14 | 0.34 | 4 | No |
| -20 1/2 | 12.1 | 1.8 | 17 1/2 | - 3 | 0.24 | 5 | No |

17 February 1966

| | | | | | | | |
|---|---|---|---|---|---|---|---|
| 76 | 6.0 | 72 | 8 | 84 | 0.82 | 25 | Yes |
| 53 | 8.1 | 69 | 11 | 64 | 0.84 | 30 | Yes |
| 11 | 10.0 | 57 | 14 | 25 | 0.75 | 10 | No |
| -25 | 15.0 | 51 | 23 | - 2 | 0.78 | 4 | No |
| -27 | 17.0 | 39 | 27 1/2 | 1/2 | 0.70 | 4 | No |
| - 1 | 3.5 | 8.9 | 4 1/2 | 3 1/2 | 0.152 | 2 | No |
| - 3 1/2 | 4.0 | 7.1 | 5 1/2 | 2 | 0.143 | 3 | No |
| - 4 | 4.5 | 4.2 | 6 | 2 | 0.123 | 3 | No |
| - 5 | 5.0 | 2.4 | 6 1/2 | 1 1/2 | 0.114 | 3 | No |
| - 8 1/2 | 5.5 | 0.5 | 7 | - 1 1/2 | 0.104 | 3 | No |

## 2.0°K Data (cont.)

17 February 1966 (cont.)

| D | Δh | v | Δ | D + Δ | $\bar{v}_s$ | ± | Filler |
|---|---|---|---|---|---|---|---|
| - 1 | 3.2 | 1.2 | 4 | 3 | 0.070 | 2 | No |
| -20 | 9.5 | 26 | 13 | - 7 | 0.43 | 3 | No |
| -25 | 11.2 | 15.8 | 16 | - 9 | 0.36 | 4 | No |
| -16 1/2 | 13.0 | 8.8 | 19 | 2 1/2 | 0.32 | 7 | No |
| -13 | 12.4 | 5.5 | 18 | 5 | 0.28 | 3 | No |
| -15 | 13.0 | 0.9 | 19 | 4 | 0.24 | 5 | No |

18 February 1966

| | | | | | | | |
|---|---|---|---|---|---|---|---|
| - 5 | 10.1 | 10.5 | 14 | 9 | 0.29 | 5 | Yes |
| -27 | 3.0 | 103 | 4 | -23 | 1.08 | 18 | No |
| -76 | 5.5 | 92 | 7 | 83 | 1.02 | 60 | Yes |
| 5 | 9.0 | 89 | 12 1/2 | 18 | 1.05 | 20 | No |
| -22 | 12.5 | 78 | 18 | - 4 | 1.01 | 10 | No |
| 36 | 7.5 | 52 | 10 | 46 | 0.66 | 20 | No |

19 February 1966

| | | | | | | | |
|---|---|---|---|---|---|---|---|
| -17 1/2 | 7.0 | 25 | 9 1/2 | - 8 | 0.38 | 5 | No |
| -14 1/2 | 9.0 | 18.6 | 12 1/2 | - 2 | 0.35 | 3 | No |
| - 5 | 11.0 | 11.2 | 15 1/2 | 10 | 0.31 | 4 | No |
| 3 1/2 | 12.5 | 6.3 | 18 | 22 | 0.29 | 4 | Yes |
| - 8 | 13.9 | 2.6 | 21 | 13 | 0.28 | 4 | Yes |
| 150 | 9.0 | 131 | 12 1/2 | 162 | 1.47 | 80 | Yes |
| 530 | 10 | 230 | 14 | 540 | 2.5 | 150 | Yes |

## 2.0°K Data (cont.)

### 19 February 1966 (cont.)

| D | Δh | v | Δ | D + Δ | $\bar{v}_s$ | ± | Filler |
|---|---|---|---|---|---|---|---|
| 148 | 9 | 140 | 12 1/2 | 160 | 1.56 | 70 | Yes |
| 420 | 8 | 222 | 11 | 430 | 2.36 | 150 | Yes |
| 1060 | 11 | 350 | 16 | 1080 | 3.7 | 200 | Yes |
| 2160 | 6 | 460 | 8 | 2170 | 4.7 | 300 | Yes |

### 8 March 1966

| | | | | | | | |
|---|---|---|---|---|---|---|---|
| 30 | 7.0 | 44 | 9 1/2 | 40 | 0.57 | 15 | Yes |
| 6 1/2 | 11.0 | 32 | 15 1/2 | 22 | 0.52 | 3 | No |
| - 4 1/2 | 14.5 | 21.9 | 22 | 18 | 0.48 | 4 | No |
| 4 | 7.2 | 82 | 10 | 14 | 0.95 | 15 | No |
| -46 | 4.7 | 82 | 6 1/2 | -40 | 0.90 | 70 | Yes |
| -34 | 5.0 | 69 | 7 | -27 | 0.78 | 45 | Yes |
| 1/2 | 3.6 | 54 | 4 1/2 | 5 | 0.60 | 4 | No |
| -32 | 15.2 | 49 | 23 1/2 | - 8 | 0.76 | 5 | No |
| -21 | 12.6 | 35 | 18 | - 3 | 0.58 | 4 | No |
| - 1 | 3.1 | 44 | 4 | 3 | 0.50 | 4 | No |
| 0 | 0.5 | 0.5 | 1/2 | 1/2 | 0.014 | 2 | No |
| - 1/2 | 1.1 | 1.3 | 1 | 1/2 | 0.033 | 2 | No |
| -15 1/2 | 14.7 | 5.7 | 22 1/2 | 7 | 0.32 | 5 | No |
| - 8 | 13.5 | 2.9 | 20 | 12 | 0.27 | 5 | No |
| - 3 | 8.2 | 6.6 | 11 | 8 | 0.214 | 3 | No |

## 2.13°K Data

27 February 1966

| D | Δh | v | Δ | D + Δ | $\bar{v}_s$ | ± | Filler |
|---|---|---|---|---|---|---|---|
| 0 | 5.2 | 0.2 | 5 1/2 | 5 1/2 | 0.28 | 1.7 | No |
| - 3 | 2.8 | 0.1 | 3 | 0 | 0.18 | 0.9 | No |
| 1 | 1.2 | 1.4 | 1 | 2 | 0.13 | 1.0 | No |
| 0 | 2.8 | 2.0 | 3 | 3 | 0.26 | 1.2 | No |
| -17 | 13.7 | 4.7 | 16 | -1 | 1.05 | 2.8 | No |
| -11 | 9.0 | 51 | 9 1/2 | -1 1/2 | 2.56 | 2.5 | No |
| - 7 | 3.0 | 1.0 | 3 | -4 | 0.23 | 1.4 | No |
| - 5 | 4.8 | 3.7 | 5 | 0 | 0.45 | 1.5 | No |
| - 3 | 4.9 | 0.9 | 5 1/2 | 2 1/2 | 0.34 | 1.6 | No |
| - 2 | 0.9 | 1.1 | 1 | -1 | 0.10 | 1.0 | No |
| -11 1/2 | 10.8 | 1.0 | 12 | 1/2 | 0.72 | 1.5 | No |
| -10 | 9.2 | 0.8 | 9 | -1 | 0.61 | 2.0 | No |
| 0 | 4.0 | 13.7 | 4 | 4 | 0.80 | 0.8 | No |
| - 7 1/2 | 5.6 | 101 | 5 1/2 | -2 | 4.40 | 2.5 | No |
| - 3 1/2 | 1.4 | 1.8 | 1 1/2 | -2 | 0.16 | 1.0 | No |

3 March 1966

| | | | | | | | |
|---|---|---|---|---|---|---|---|
| -17 | 9.9 | 4.2 | 11 | -6 | 0.79 | 3.5 | No |
| -12 | 12.1 | 18.7 | 14 | 2 | 1.51 | 3.0 | No |
| 0 | 4.9 | 45 | 5 | 5 | 2.12 | 1.3 | No |
| -15 | 13.0 | 64 | 15 | 0 | 3.38 | 4.0 | No |
| - 4 | 5.8 | 2.9 | 6 1/2 | 2 1/2 | 0.48 | 1.7 | No |

## 2.15°K Data

28 February 1966

| D | Δh | v | Δ | D + Δ | $\bar{v}_s$ | ± | Filler |
|---|---|---|---|---|---|---|---|
| - 2.6 | 3.9 | 4.1 | 4.4 | 1.8 | 0.60 | 2 | No |
| - 3.6 | 5.5 | 6.9 | 6.6 | 3.0 | 0.94 | 2 | No |
| - 11.0 | 7.8 | 9.8 | 10.3 | - 0.7 | 1.33 | 2 | No |
| - 9.2 | 9.0 | 2.0 | 12.5 | 3.3 | 0.94 | 3 | No |
| - 14.8 | 11.5 | 5.9 | 16.9 | 2.1 | 1.41 | 3 | No |
| - 7.3 | 3.8 | 23.0 | 4.0 | - 3.3 | 1.79 | 3 | No |
| - 14.7 | 7.2 | 10.7 | 9.3 | - 5.4 | 1.34 | 2 | No |
| - 16.5 | 11.8 | 10.0 | 17.7 | 1.2 | 1.69 | 4 | No |
| - 55 | 2.5 | 50 | 2.8 | - 52 | 3.37 | 20 | No |
| - 7.3 | 2.7 | 42 | 2.8 | - 4.5 | 2.87 | 9 | No |
| - 3.7 | 3.5 | 15.0 | 3.8 | 0.1 | 1.26 | 4 | No |
| - 55 | 2.9 | 45 | 3.1 | - 52 | 3.10 | 17 | No |
| - 36.6 | 6.0 | 38 | 7.2 | - 29.4 | 2.93 | 6 | No |
| - 18.3 | 9.9 | 17.7 | 13.7 | - 4.6 | 2.02 | 3 | No |
| -110 | 5.1 | 60 | 5.8 | -104 | 4.50 | 30 | No |
| - 37 | 7.2 | 40 | 9.0 | - 28 | 3.17 | 8 | No |
| - 44 | 8.3 | 35 | 11.0 | - 33 | 3.13 | 7 | No |
| - 44 | 10.0 | 30 | 13.8 | - 31.2 | 2.79 | 7 | No |
| - 18.3 | 2.0 | 24.8 | 2.0 | - 16.3 | 1.76 | 5 | No |
| - 7.3 | 5.2 | 14.2 | 6.2 | - 1.1 | 1.35 | 2 | No |
| -204 | 5.0 | 65 | 5.9 | -198 | 6.02 | 40 | No |
| -110 | 6.0 | 65 | 7.2 | -103 | 4.64 | 30 | No |
| - 14.7 | 9.0 | 11.9 | 12.3 | - 2.4 | 1.57 | 3 | No |

## 2.15°K Data (cont.)

28 February 1966

| D | Δh | v | Δ | D + Δ | $\bar{v}_s$ | ± | Filler |
|---|---|---|---|---|---|---|---|
| -14.7 | 9.9 | 8.9 | 13.9 | - 0.8 | 1.46 | 3 | No |
| - 7.3 | 1.9 | 16.6 | 4.8 | -25 | 1.46 | 2 | No |
| 1.8 | 2.0 | 16.4 | 2.0 | 3.8 | 1.19 | 4 | No |
| -22.0 | 6.0 | 21.2 | 7.8 | -14.2 | 1.89 | 3 | No |
| -92 | 10.5 | 40 | 15.0 | -77 | 3.47 | 8 | No |

## 2. 163°K Data

4 March 1966

| D | Δh | v | Δ | D + Δ | $\bar{v}_s$ | ± | Filler |
|---|---|---|---|---|---|---|---|
| - 1 | 0.7 | 0.3 | 1 | 0 | 0.21 | 5 | No |
| -16 | 6.4 | 9.3 | 7 | - 9 | 2.95 | 6 | No |
| -32 | 4.7 | 23.6 | 5 | -27 | 4.96 | 6 | No |
| -27 | 2.0 | 20.4 | 2 | -25 | 3.72 | 6 | No |
| -72 | 4.1 | 32.4 | 4 | -68 | 6.12 | 12 | No |
| -43 | 9.8 | 11.4 | 13 | -30 | 4.02 | 8 | No |
| -72 | 10.4 | 24.5 | 13 | -59 | 6.31 | 11 | No |
| -69 | 8.1 | 23.2 | 10 | -59 | 5.58 | 14 | No |
| - 2 | 3.2 | 6.9 | 3 | 1 | 1.85 | 5 | No |